energies

MDPI

Review

A State-of-the-Art Review on Coupling Technology of Coal-Fired Power and Renewable Energy

Yulan He [1,2], Ziqu Ouyang [1,2,*], Hongliang Ding [1,2,*], Hongshuai Wang [1,2], Shuyun Li [1,2] and Lingming Wu [1,2]

[1] State Key Laboratory of Coal Conversion, Institute of Engineering Thermophysics, Chinese Academy of Sciences, Beijing 100190, China; heyulan@iet.cn (Y.H.); wanghongshuai@iet.cn (H.W.); lishuyun@iet.cn (S.L.); wulingming@iet.cn (L.W.)
[2] University of Chinese Academy of Sciences, Beijing 100049, China
* Correspondence: ouyangziqu@iet.cn (Z.O.); dinghongliang@iet.cn (H.D.); Tel.: +86-10-82544448 (Z.O.); Fax: +86-10-82543191 (H.D.)

Abstract

The Paris Agreement and related international climate frameworks aim to reduce global carbon intensity; however, carbon dioxide emissions from electricity generation remain high, motivating the development of coal–renewable coupling technologies to lower the carbon intensity of power production. Coal–renewable coupling refers to the technical integration of conventional coal-fired power systems with renewable energy sources such as wind and solar to form a synergistic and complementary energy supply system. At present, systematic reviews and comprehensive analyses of coal–renewable coupling technologies are still limited. Accordingly, this paper categorizes existing approaches into two pathways—deep flexible load regulation and co-firing-based emission reduction—and systematically reviews the current state of technological development, identifies key challenges, and discusses potential future directions. Deep flexible load regulation includes flexibility retrofitting of coal-fired units and the integration of energy storage modules, whereas co-firing-based emission reduction mainly involves the co-combustion of coal with zero-carbon fuels. The analysis focuses on large-scale coal-fired units, covering low-load stable combustion technologies, steam turbine retrofitting, and rapid start-up and shutdown strategies. For energy storage-assisted load regulation, both conventional options and emerging technologies such as molten salt and high-temperature solid particle thermal energy storage are examined. Zero-carbon fuels considered include biomass, ammonia, and hydrogen. Furthermore, the economic feasibility of the various technologies is evaluated, providing reference value for deep flexibility retrofitting and substantial emission reduction in large-scale coal-fired power plants.

Keywords: coal-fired power; renewable energy; flexibility retrofitting; energy storage; zero-carbon fuels

Check for updates

Academic Editor: Changkook Ryu

Received: 19 November 2025
Revised: 16 December 2025
Accepted: 23 December 2025
Published: 29 December 2025

Copyright: © 2025 by the authors. Licensee MDPI, Basel, Switzerland. This article is an open access article distributed under the terms and conditions of the Creative Commons Attribution (CC BY) license.

1. Introduction

With the adoption and continued implementation of the Paris Agreement, together with related international climate frameworks and agreements, the international community is advancing the reduction of carbon dioxide emissions with unprecedented intensity. The carbon intensity of the power sector has long remained at a relatively high level, and electricity demand is expected to further increase as emerging economies continue to develop. According to statistics from the International Energy Agency, carbon dioxide emissions from electricity generation in 2024 amounted to approximately 13.8 billion tonnes,

remaining the highest among all sectors [1]. Meanwhile, owing to differences in national energy endowments, coal-fired power plants still constitute the backbone of electricity generation in many countries. Coal combustion not only emits carbon dioxide but also releases air pollutants such as NO_x and SO_2, making the selection of appropriate flue-gas desulfurization technologies particularly critical [2]. Consequently, achieving simultaneous carbon reduction and pollution abatement in the power sector, especially in coal-fired power plants, has become an urgent technological challenge that must be addressed.

To reduce the carbon intensity of electricity production, many countries have begun to expand the deployment of renewable energy for power generation and to progressively increase its share in the electricity mix. In 2025, U.S. power producers plan to retire 12.3 GW of generation capacity, of which coal-fired power accounts for the largest share of planned retirements at 66%, followed by natural gas at 21%, while an additional 63 GW of utility-scale capacity is expected to be commissioned, with solar power and battery energy storage together representing 81% of the projected capacity additions [3]. In 2024, the share of renewable electricity generation in the European Union reached 47%, an increase of 2.6 percentage points compared with 2023 [4]. In 2024, the combined share of large-scale hydropower, nuclear power, wind power, and solar power in China's above-scale industrial electricity generation rose to 32.6% [5].

However, as the share of renewable electricity generation continues to increase, the associated technical challenges have become increasingly pronounced. High penetrations of renewable energy exhibit strong intermittency and stochasticity, posing significant challenges to the secure and stable operation of power systems and leading to rising levels of wind and solar curtailment. Under extreme weather conditions, renewable power generation is highly likely to be disrupted or suspended, highlighting the limited resilience of systems relying solely on renewable energy. At the same time, the frequent occurrence of negative electricity prices, as shown in Table 1 [6], has substantially undermined the incentives of power producers and the functioning of electricity spot markets.

Table 1. Occurrence of negative electricity prices in selected regions in 2024 [6].

Comparison Project	Share of Installed Wind and Solar Capacity	Peak Frequency of Negative Electricity Prices
Germany	58%	9.65%
Australia	50.2%	38.82%
Shandong Province, China	46.9%	48.09%
Zhejiang Province, China	36.8%	75% (during the Spring Festival)

Climate change poses an urgent challenge, and the large-scale deployment of renewable electricity generation is therefore inevitable; however, this does not imply the complete phase-out of coal-fired power plants, but rather a transition of coal power from a "baseload" role to a "flexibility-providing" or "balancing" resource to accommodate renewable variability and ensure the secure and stable operation of power systems. Against this backdrop, coupling technologies between coal-fired power and renewable energy have been proposed, referring to the integrated combination of conventional coal-based generation systems with renewable sources such as wind and solar through technical measures to form a synergistic and complementary energy supply system. In recent years, approaches to coupling coal-fired power with renewable energy have diversified globally, encompassing coordinated dispatch of "coal power plus renewables" within power systems, flexibility retrofitting of

coal-fired units, the integration of emerging energy storage technologies, and co-firing of coal with zero-carbon fuels.

Flexibility retrofitting of coal-fired power units enhances their wide-load operating capability, enabling deep and flexible load regulation of coal-fired boilers, thereby allowing power systems to maximize the integration of renewable electricity generation; at present, retrofitted coal-fired units can achieve stable operation at minimum loads as low as 20% of rated capacity [7]. Energy storage systems represent an effective means of addressing the variability of renewable energy and can also reduce wind and solar curtailment; Yang et al. [8] maintained power balance after grid integration of wind and photovoltaic generation by incorporating battery energy storage systems (BESS). Co-firing of zero-carbon fuels with coal can effectively reduce CO_2 emissions while maintaining power system stability, and this technology has been the subject of active research in many countries. In the United States, woody biomass has been co-fired in fossil-fuel-based power generation platforms to reduce the share of fossil fuel consumption [9].

Coupling technologies between coal-fired power and renewable energy are widely recognized as one of the key pathways for the energy transition, with many countries and regions promoting their coordinated development through policy guidance and international cooperation. China leverages the catalytic role of government investment to encourage regions to formulate locally tailored support policies and to increase investment subsidies for low-carbon retrofitting and construction projects of coal-fired power plants [10]. The North American Renewable Integration Study has proposed that cross-regional power transmission and coordination can enable more effective utilization of renewable energy while employing coal-fired power as a backup resource to ensure the stable operation of power systems [11].

At present, a wide range of technologies and concepts have been proposed to enable the coupling of coal-fired power with renewable energy; however, most review studies focus only on selected approaches, lack a comprehensive analysis spanning the combustion side, steam cycle, and grid interface, provide limited discussion of emerging technologies, and adopt relatively fragmented classification schemes, which hinders systematic understanding and the synthesis of innovations. Accordingly, this paper broadly categorizes coal–renewable coupling strategies into two main pathways: deep flexible load regulation and co-firing-based emission reduction, where deep flexible load regulation encompasses flexibility retrofitting of coal-fired units and the introduction of energy storage technologies on the generation side, while co-firing-based emission reduction primarily involves the co-combustion of coal with zero-carbon fuels. The current development status of relevant technologies worldwide is systematically reviewed, the key technical challenges associated with each pathway are analysed, potential future development directions are identified and discussed, and the economic feasibility of the different technologies is also evaluated. This work aims to contribute to global carbon mitigation efforts, support low-carbon transitions in coal-fired power plants, and promote the sustainable development of the energy sector.

2. Current Status of Flexibility Retrofitting Technologies for Coal-Fired Power Units

The intermittency and variability of renewable energy generation require coal-fired units to participate frequently in peak-shaving dispatching to accommodate this. Thus, enhancing the flexibility and regulating capacity of coal-fired units has become a critical measure to advance energy structure transformation and ensure stable grid operation. However, coal-fired boilers face a series of issues during peak-shaving, including reduced thermal efficiency, elevated NO_x emission concentrations [12], combustion instability, and high thermal inertia. In response to these issues, this paper focuses on research progress

in key technologies such as operational stability at minimum load, burner optimization, steam-side retrofitting, and rapid start-up and shutdown of coal-fired units.

2.1. Low-Load Stable Combustion Technology

A critical prerequisite for enhancing the flexibility of coal-fired units is that both the boiler combustion side and the steam turbine steam side can maintain safe and stable operation under low-load conditions. Low-load operation of boilers faces numerous issues, including increased coal consumption, poor combustion stability, unstable hydrodynamic conditions, and difficulties in the normal operation of flue gas pollutant purification equipment [13]. Technologies such as optimization of combustion performance, pulverized coal stable combustion burners, combustion-supporting measures, and optimization of steam turbine systems can enable boilers to achieve stable combustion under low-load conditions, ensuring the safe operation of the units.

2.1.1. Optimization of Combustion Performance

Adjusting burner operation strategies, improving pulverized coal fineness, optimizing boiler air distribution, and other such measures can all enhance combustion performance under low-load conditions to a certain extent.

Chen et al. [14] investigated the influence of variations in pulverized coal fineness on the combustion characteristics of high-ash bituminous coal. Combined with boiler low-load stable combustion tests, their findings showed that when the fineness R90 of high-ash bituminous coal pulverized coal decreased from 23% to approximately 10%, the boiler's minimum stable combustion load dropped from 35% to 30%. This indicates that reducing pulverized coal fineness can enhance the boiler's stable combustion capability under low-load conditions. Liu et al. [15] analysed the impact of different pulverizer combinations on the operational economy and safety of lignite-fired boilers. The results showed that when three pulverizers are in operation, indices such as NO_x concentration at the SCR inlet, operational safety of the coal pulverizing system, wall temperature, and operational economy are all superior to those when four pulverizers are in operation. Furthermore, when the boiler is adjusted to operate with two pulverizers, the unit can still maintain stable combustion for a short period without instantaneous flameout. To address the issue of unplanned boiler outages caused by unstable combustion at low loads, increasing the number of operating pulverizers from two to three can facilitate the stable operation of a 350 MW supercritical unit at 30% load [16].

Finer pulverization of coal can enhance the stability of combustion under low-load conditions to a certain extent; however, the minimum oil-free load is generally limited to 30~40%, making further breakthroughs difficult to achieve. Therefore, research on low-load stable combustion has largely focused on burner improvement, addition of combustion-supporting measures, and development of novel combustion technologies.

2.1.2. Pulverized Coal Stable Combustion Burner

During low-load combustion, a significant reduction in pulverized coal concentration increases ignition difficulty and weakens the recirculation zone's capacity to entrain high-temperature flue gas, thereby exacerbating combustion instability. Since operational optimization adjustments offer limited contribution to promoting stable combustion, optimized burner design is required to address these issues.

Large-scale coal-fired units in China predominantly adopt swirl combustion technology. Song et al. [17] conducted research on the combustion stability performance of swirl-type pulverized coal burners. Their results show that measures such as enhanced pulverized coal concentration and intensified high-temperature flue gas recirculation can effectively improve low-load combustion stability and enhance combustion-side peak-

shaving capability. Separately, Huang et al. [18], while retaining the burner's secondary air structure, integrated central coal feeding technology, introduced swirling slit air, and along with optimization of the premixing section and divergent outlet, achieved stable combustion at 30% load relying solely on the inherent recirculation zone. Building on the low-NO_x axial swirl burner, Wang et al. [19] added a central primary air duct for coal injection, an interstitial air duct and interstitial air vanes, and incorporated a three-stage concentrator ring inside the primary air duct. The structural configuration is shown in Figure 1.

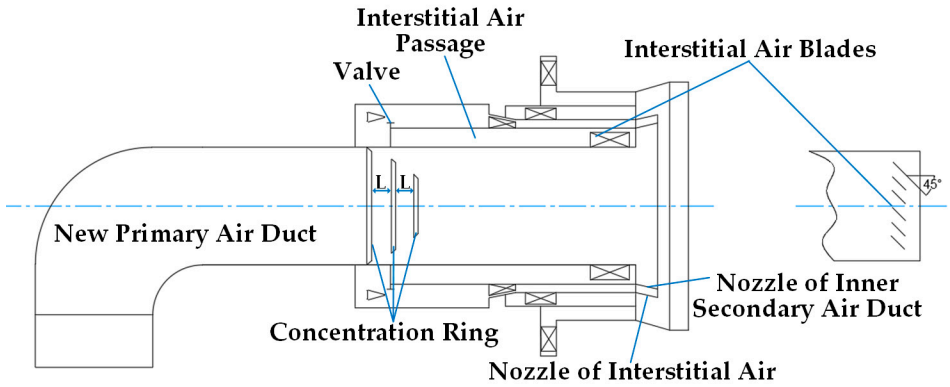


Figure 1. Structural diagram of the central coal feed swirl burner [19].

2.1.3. Combustion-Supporting Measures

Oil injection for combustion support is a common method for low-load units to achieve stable combustion. However, this method has the issue of increased local heat release and generates polluting gases. Thus, industrially, combustion-supporting methods such as micro-oil (gas) combustion support and plasma flame stabilization are widely adopted.

After pulverization, fuel oil forms a larger specific surface area, enhancing mixing with air and enabling more complete combustion. Micro-oil ignition technology facilitates rapid initiation of combustion, improves boiler combustion efficiency and stability, and reduces fuel waste and pollutant emissions [20]. Wei et al. [21] successfully ignited pulverized coal during the cold-start process of the boiler by adjusting the pulverizing system, burner secondary air dampers, and micro-oil system combustion-supporting dampers. Yang et al. [22] applied micro-oil ignition technology, achieving a fuel savings rate of over 40% single ignition, with significant economic benefits.

Plasma ignition technology can generate extremely high-temperature zones within boilers via plasma, directly igniting pulverized coal to achieve stable combustion. Compared with traditional ignition methods, this technology features higher economic efficiency and safety, and has been widely applied in various power plants. Zhang et al. [23] established a single-head swirl combustion experimental setup and studied the ignition and combustion characteristics of gliding arc plasma at the combustion chamber head. The results showed that gliding arc plasma ignition altered the ignition and combustion process of the conventional combustion chamber and expanded its stable combustion range, with the maximum expansion of the ignition limit reaching 36.7% and that of the extinction limit reaching 83.4%. Moreover, this technology increased the area of the combustion reaction zone, reduced fragments in the reaction zone, and enlarged the combustion initiation angle. Aliya Askarova et al. [24] employed 3D computer modeling methods to conduct numerical simulation experiments on boilers under operating conditions. The results showed that plasma technology can reduce the concentrations of CO and NO_x at the furnace outlet, and verified the feasibility of applying plasma ignition technology to practical thermal power generation equipment. Li et al. [25] developed a plasma ignition pulverized coal burner

with an offset concentrated slit-type pulverized coal feeding multi-stage cylinder structure, as illustrated in Figure 2, and conducted variable-condition oil-free plasma ignition tests on a 660 MW lignite-fired boiler with a total inherent moisture content of 35~40%. The results showed that this novel plasma ignition system could ignite high-moisture lignite with a calorific value of 10,900~13,400 kJ/kg, enabling oil-free start-up of the unit and exhibiting strong ignition capability. However, coking and burnout on the burner wall tend to occur when burning non-design coal types.

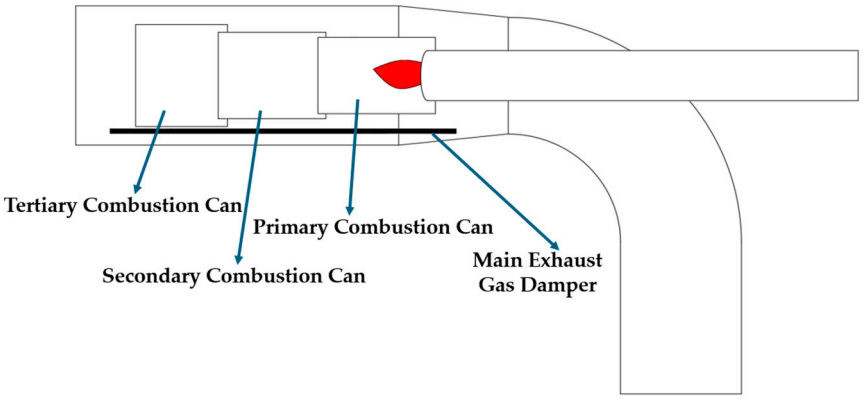


Figure 2. Model of high moisture lignite plasma burner [25].

However, current plasma ignition and flame stabilization technologies are mainly applicable to high-volatile lignite and bituminous coal, while for low-volatile lean coal and anthracite, it is difficult to effectively maintain stable low-load combustion. Furthermore, plasma electrodes exhibit poor adaptability to complex combustion environments with multiple coal types and have a limited-service life [26].

2.1.4. Novel Combustion Technology

Pulverized coal preheating combustion technology, a novel combustion technology proposed and developed by the Institute of Engineering Thermophysics, Chinese Academy of Sciences, addresses issues such as difficult ignition and slow response under low-load conditions through fuel preheating modification [27]. Moreover, this technology is applicable to the construction and retrofitting of both industrial boilers and power plant boilers, featuring strong fuel adaptability, low NO_x emissions, and flexible load adjustment. It is one of the peak-shaving methods with great development potential.

The key component of preheating combustion technology is the preheating burner. The burner proposed by the Institute of Engineering Thermophysics, Chinese Academy of Sciences features a circulating fluidized bed (CFB)-like structure, leveraging its advantages of high combustion efficiency and uniform combustion in the "fluidized state" to achieve fluidized thermal modification of fuel. Its principle is illustrated in Figure 3 [28]: Pulverized coal undergoes partial combustion to release heat in a fluidized preheating burner, achieving fuel modification to form a high-temperature gas-solid mixed fuel containing coal gas and highly reactive semi-coke, which then enters the furnace for suspension combustion. After preheating modification, the pulverized coal has a reduced particle size, with significantly increased specific surface area and active sites of particles, and a temperature higher than its ignition temperature. It exhibits distinct gaseous fuel combustion characteristics, rapidly combusting upon entering the furnace, thus realizing the "quasi-gasification" of solid fuel and breaking through the challenges of flexible combustion and stable low-load combustion of pulverized coal. Meanwhile, the strongly reducing atmosphere in the preheating burner enables the nitrogen element released during preheating to be directionally reduced to N_2, thereby significantly reducing NO_x formation in the furnace [27].

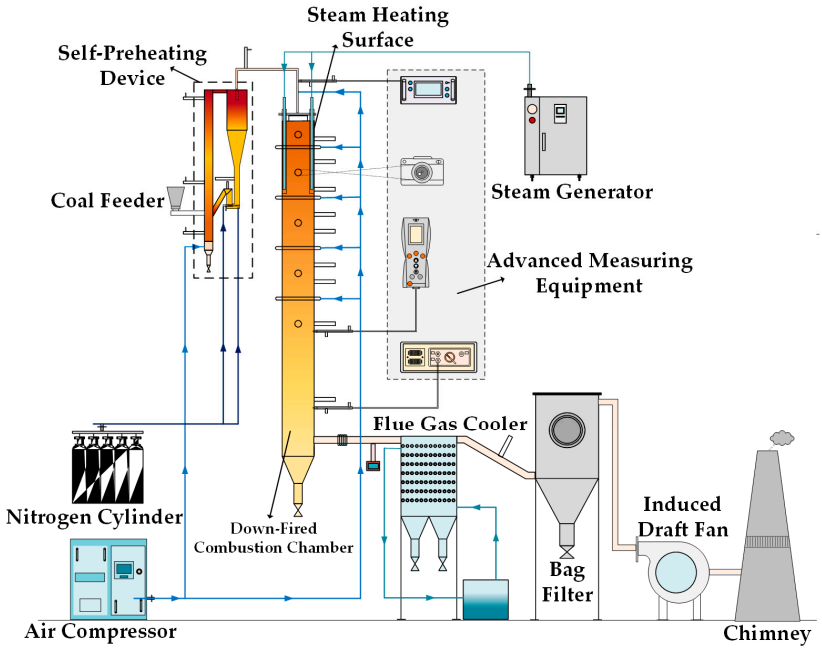


Figure 3. Schematic diagram of kW-level pulverized coal preheating combustion flexible peak shaving test system [28].

For this type of preheating burner, researchers have conducted extensive relevant experimental studies and optimization-improvement work. Wang et al. [28] proposed using the combustion temperature on the combustion side and steam parameters on the working fluid side as dual criteria for judging load variation stability. The study found that: the fluidized preheating combustion technology enables coal-fired boilers to operate stably within the 25~110% load range, and the NO_x emissions during operation are consistently controlled below 300 mg/m^3, which is 35~40% lower than that of traditional combustion methods. Hui et al. [29] conducted a systematic study on the thermal modification characteristics and variable-load operation characteristics of four typical types of coal based on preheating combustion technology. The results showed that: Alashan Youqi lignite, Shenmu bituminous coal, Ruiguang lean coal, and Sihe anthracite could operate stably within the unit load ranges of 25~110%, 25~113%, 35~110%, and 40~105%, respectively. This confirms that the CFB type preheating combustion technology has coal-type adaptability and can effectively adapt to power grid peak-shaving conditions. Ding et al. [30] conducted a systematic investigation on the combustion performance and NO_x emission characteristics of low-quality coal (LQC) under wide-load conditions on an MW-grade pilot-scale test platform. Employing the fluidized preheating-based fuel modification technology, they successfully achieved the safe and stable operation of LQC at a 20% load without any auxiliary energy input. Zhu et al. [31] first adopted the technical route of CFB coupled with pulverized coal preheating, completed the retrofitting of a 240 t/h CFB boiler, and realized its successful operation. The test results show that: the boiler load can be deeply adjusted from 50% (before retrofitting) to 32%; and when the preheating burner is put into operation under the 50% load condition, the unit can directly achieve ultra-low NO_x emissions under the condition of zero ammonia injection, with the NO_x emission concentration being only 29 mg/m^3.

Besides the pulverized coal preheating-modified combustion technology, other novel combustion technologies also include gasification-coupled combustion technology, self-preheating burners, and internal-combustion burners, among others.

The Institute of Coal Chemistry, Chinese Academy of Sciences (CAS) has developed a coal gasification-coupled stable combustion technology for pulverized coal-fired boilers

under low load. This technology has achieved stable operation at 20% load on the 350 MW unit of Jinkong Electric Power Hejin Power Generation Branch (Hejin, China), thereby having realized for the first time the deep peak-shaving operation of pulverized coal-fired boilers firing lean coal under low load [32].

Zhang et al. [33] have developed a self-preheating pulverized coal burner with high coal concentration (as illustrated in Figure 4), and have designed a separation sleeve inside the burner, between the primary air and secondary air, to enhance the formation of the recirculation zone. The research team has applied this self-preheating burner to a 29 MW coal-fired industrial boiler and conducted industrial-scale tests. The results show that under an ultra-low load condition of approximately 13%, the boiler can achieve a stable combustion efficiency of 93.24%, with a NO_x emission concentration of about 43.6 mg/m^3, exhibiting excellent NO_x reduction performance.

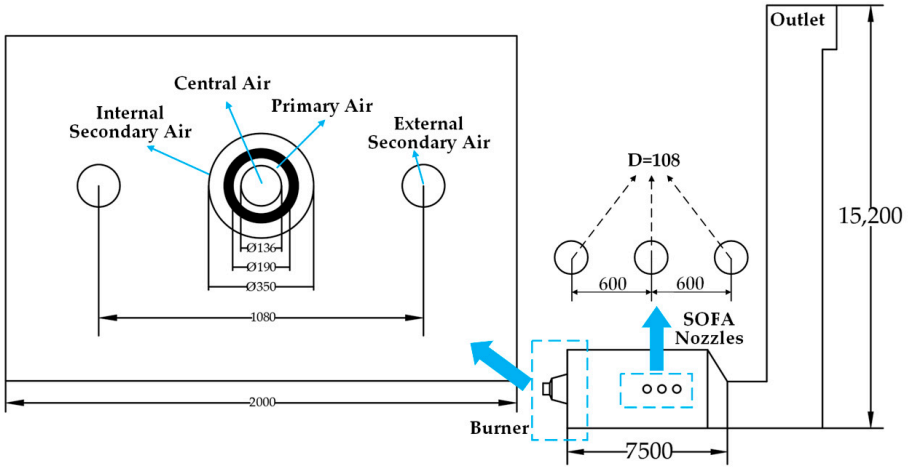


Figure 4. The structure of self-preheating pulverized coal burner [33]. (All dimensions are in mm).

Yao et al. [34] have adopted a numerical simulation method to investigate, for a 600 MW tangentially fired boiler, the retrofit effect of internal combustion burners (whose structure is illustrated in Figure 5) based on the pulverized coal preheating method, as well as the law of syngas generation. The results show that at the burner outlet, the volume fractions of CH_4, CO, and H_2 in the syngas are 0.95%, 12.7%, and 0.8%, respectively. Under this strongly reducing atmosphere, the volatile nitrogen and char nitrogen released from the pulverized coal can be directly converted into N_2; meanwhile, the preheating of pulverized coal advances the ignition position inside the furnace, enhances the flame jet intensity, and thus improves combustion stability under low-load conditions.

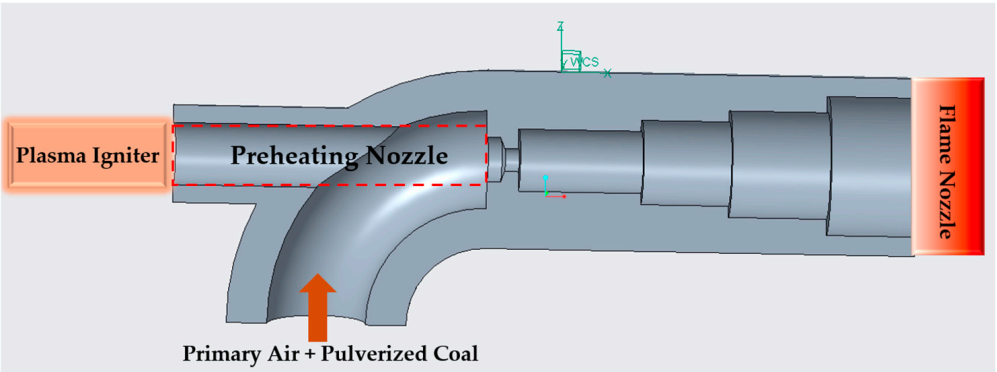


Figure 5. Internal combustion burner structure [34].

In summary, novel combustion technologies can significantly improve the combustion stability of coal-fired units under low load and their response rate to load changes, while effectively reducing NO_x emissions. However, at the current stage, the requirements for coal-fired units regarding the depth of flexible peak shaving, load regulation range, and load response capability have been further increased. Meanwhile, research on the ultra-low load performance of novel combustion technologies remains focused on the stages of laboratory R&D and pilot-scale verification, with a lack of large-scale demonstration projects and engineering application cases. Therefore, in-depth research and innovative optimization for the engineering application of novel combustion technologies are urgently needed.

2.1.5. Oxygen-Enriched Combustion Technology

Oxygen-enriched combustion is an efficient and clean combustion technology that uses oxygen-enriched gas with an oxygen content exceeding 21% (typically 25~35% or even higher) to replace ambient air as the oxidizer. This technology can increase the combustion temperature, enhance heat transfer efficiency, lower the fuel ignition temperature [35], and improve combustion stability under low-load conditions. Meanwhile, the CO_2 concentration in the flue gas generated after combustion is relatively high; after treatment, the CO_2 in the flue gas can be directly compressed for storage or utilization, which effectively reduces the cost of carbon capture.

Skryja et al. [36] investigated the effect of oxygen-enriched conditions on the combustion process and found that premixed oxygen-enriched combustion could achieve stable flame combustion under low-power combustion operating conditions. Tian et al. [37] carried out experiments on oil-free stable combustion under low load and oxygen-injection enhanced stable combustion for a 300 MW tangentially fired boiler. The experimental results showed that under the operating conditions of oil-free stable combustion and oil-free stable combustion combined with oxygen injection, the minimum stable combustion loads of the boiler were 106 MW and 60 MW, respectively; based on the 300 MW rated load of this boiler, the minimum stable combustion load decreased from 35% to 20% after oxygen injection. Lun et al. [38] analyzed the effect of primary air oxygen concentration on the co-combustion characteristics of furnace gas and pulverized coal in a rotary kiln based on the computational fluid dynamics (CFD) method. The simulation results showed that when the primary air oxygen concentration increased from 21% to 37%, the pulverized coal combustion rate increased significantly, the roasting zone length increased from 18.2 m to 20.9 m, and the flame peak temperature rose from 1999 K to 2149 K, but the NO_x formation amount increased simultaneously. It is worth noting that the NO_x emission growth rate when the oxygen concentration increased from 21% (corresponding to a NO_x emission of 319.5 mg/m^3) to 29% (corresponding to a NO_x emission of 380.7 mg/m^3) was much lower than that when it increased from 29% to 37% (corresponding to a NO_x emission of 506.9 mg/m^3). Therefore, the optimal primary air oxygen concentration for the rotary kiln under its operating conditions can be determined through synergistic optimization that integrates the combustion enhancement effect and NO_x emission control requirements.

Traditional oxygen-enriched combustion technology suffers from issues such as high energy consumption and high operating costs [39]. As its technical optimization route, pressurized oxygen-enriched combustion technology achieves outcomes including enhancement of system net efficiency [40], reduction in the scale of carbon capture equipment, and decrease in carbon capture cost [41] by increasing combustion pressure; therefore, it is regarded as one of the most promising carbon capture solutions for coal-fired power plants in industrial development [42]. In terms of technical verification, the staged pressurized oxygen-enriched combustion technology independently developed by the Institute of Engineering Thermophysics, CAS has completed megawatt-scale pilot verification, successfully

achieving 72 h of continuous and stable operation under a pressure of 1.0 MPa, with the CO_2 concentration in dry flue gas reaching over 93% during the test [43]. Despite the aforementioned progress, the current pressurized oxygen-enriched combustion technology is still in its initial stage, facing problems such as scarcity of large-scale demonstration projects and insufficient industrial application experience, which urgently require further in-depth research and technical optimization.

2.2. Steam Turbine System Retrofitting

As the share of renewable energy generation continues to increase, the participation of coal-fired power units in deep peak shaving has become a regular operational practice. Steam turbines often operate under low-load or even extremely low-flow conditions, which can lead to issues such as excessive thermal stress, delayed regulation response, component wear, and erosion of the last-stage blades in steam turbines. Currently, research on the optimization and retrofitting of steam turbines mainly focuses on enhancing control systems, improving internal structures, and optimizing water-steam systems.

Optimizing control strategies can enhance the load-following responsiveness of steam turbines and mitigate the adverse effects on the steam turbine itself caused by inappropriate control strategies under low-load operation. Xing [44] proposed key technologies for the steam turbine control system of ultra-supercritical units, including the optimization of dynamic characteristics for the turbine-boiler coordinated control system, the dynamic characteristic compensation of steam admission control valves for the high-pressure cylinder, and the online monitoring of rotor thermal stress. After the application of these technologies to unit retrofitting, the research results showed that compared with the pre-retrofitting period, the unit's load adjustment rate increased by approximately 25%, the peak value of main-steam pressure fluctuation decreased by about 44.2%, the response speed to automatic generation control commands improved by 35.7%, and the fault switching time of the linear variable differential transformer was shortened by roughly 48.6%. Zhu et al. [45] applied deep reinforcement learning technology to the field of steam turbine intelligent control optimization, proposed a main steam temperature controller based on the twin delayed deep deterministic policy gradient (TD3) algorithm, the algorithmic framework is shown in Figure 6. Verified by simulation calculations, the cold start-up time and warm start-up time of the unit were shortened by approximately 3.7% and 2.9%, respectively. On the premise of ensuring unit operational safety, this technology effectively improved the unit start-up speed.

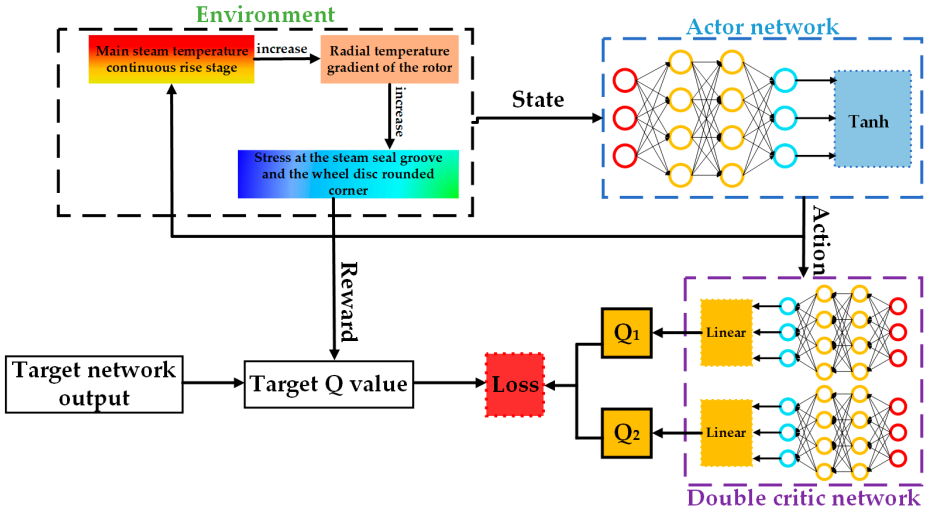


Figure 6. Algorithmic framework for the TD3-MSTC control model [45].

Steam turbine blades are core components that convert steam kinetic energy into mechanical energy. Under deep peak shaving conditions, the flow characteristics of the flow field in the steam turbine's low-pressure (LP) cylinder are complex, with various vortices generated [46] and significant temperature variations occurring. In particular, the last-stage and second-last-stage blades are prone to water erosion, which alters their surface roughness and leads to blade fracture [47]; other issues include last-stage blade flutter [48,49], steam backflow, among others. To enhance the operational stability and safety of steam turbines under low-load conditions, scholars have proposed methods such as improving component materials and structures, strengthening last-stage blades via thermal spraying, and adjusting the outlet pressure of the last stage within the LP cylinder. Han et al. [46] employed a three-dimensional numerical simulation method to investigate the non-equilibrium flow characteristics of wet steam in the last two stages of a 300 MW steam turbine, revealed the flow instability mechanism under low-flow conditions, and further proposed a dynamic backpressure optimization method as shown in Figure 7. The research results show that: under the 30% turbine heat acceptance (THA) condition, when the backpressure is reduced from 4.9 kPa to 2.1 kPa, the backflow vortices in the exhaust passage are completely dissipated, the streamlines tend to be parallel, and the flow state is significantly optimized; under the 20% THA condition, reducing the backpressure to 3.5 kPa can eliminate the tip clearance vortices between the last-stage stator and rotor blades, and when further reduced to 2.1 kPa, the vortices in the flow passage almost completely disappear, allowing smooth steam flow; however, under the 10% THA condition, due to the extremely low unit flow rate, although reducing the backpressure can narrow the vortex area, it cannot completely eliminate the adverse pressure gradient, and partial backflow vortices still exist in the flow passage. Mei et al. [50] conducted supersonic flame spraying (SFS) tests on the last-stage blades of steam turbines. It was found that the SFS-sprayed coating had a dense and homogeneous surface with no obvious visible defects; the coating thickness ranged from 0.15 to 0.25 mm, the porosity was less than 2%, the hardness exceeded 800 HV0.3, and the adhesion strength was greater than 70 MPa. These results confirm that the SFS technology has a significant effect on improving the water erosion resistance of the material. Abdullah et al. [51] conducted a study on protecting turbine blades by adding metals to ceramic materials via the flame spraying method. The test results showed that when the composite system was Al_2O_3-%Fe-%Cu, under specific process conditions (spray angle of 90°, spray distance of 15 cm, and sintering at 1100 °C for 2 h), and the Cu addition ratio was 25%, the prepared coating exhibited the optimal performance.

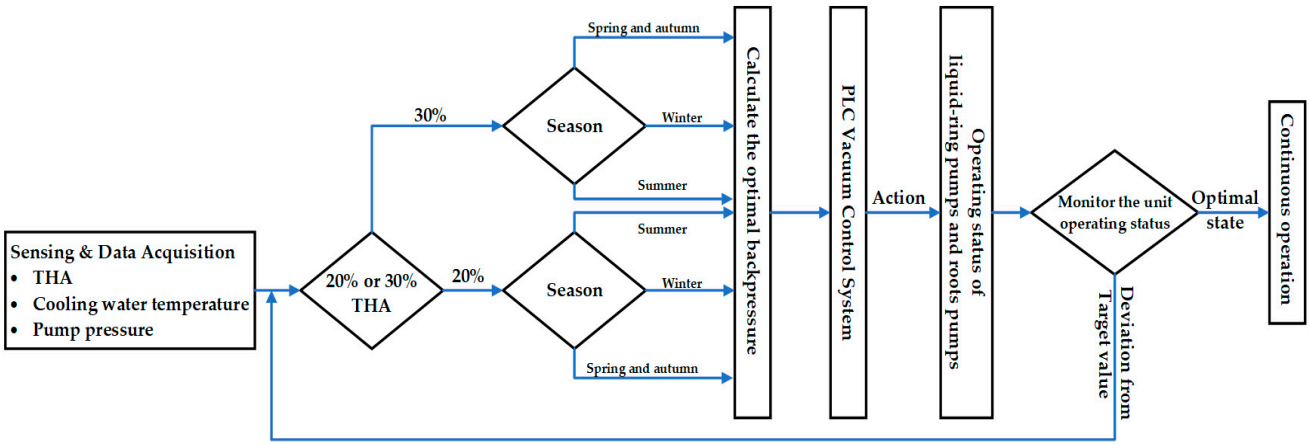


Figure 7. Logic diagram of the dynamic backpressure optimization method [46].

Optimizing the state and transportation of the water-steam medium and ensuring the stability of its parameters can indirectly create conditions for the safe and efficient operation of steam turbines. Tong et al. [52] conducted experimental research and numerical simulation on the stable combustion performance of a subcritical forced-circulation tangentially fired (four-corners) boiler under ultra-low load (20% rated load). The research results show that under the operating conditions of 20~50% rated load, the tube wall temperatures of the superheater and reheater can all be stably controlled below the alarm threshold; however, during the dynamic processes of unit load ramp-up and ramp-down, overtemperature of the superheater's divided platens and rear platens tends to occur. For the retrofitting project of Guoneng Jiangsu Jianbi Power Plant [53], the "flexible regenerative heating" energy-saving technology was adopted, combined with boiler combustion optimization, flue gas-air system optimization, and steam injection heat pump technology. This significantly reduced the net coal consumption for power generation under the 20% deep peak shaving condition. The unit's load adjustment range is 15~100% of the rated power, the average load ramp rate stands at 2.5% Pe/min, and the net coal consumption for power generation at 20% load is reduced by 20 g/kWh.

To further enhance the depth of peak shaving and achieve stable operation under ultra-low load (below 20%), a variety of new technologies are developing vigorously, among which the near-zero output of the steam turbine's LP cylinder is one of the key retrofitting technologies. This technology can partially free up the peak-shaving capacity of the unit, with its operating principle illustrated in Figure 8 [54,55]. Lu et al. [56] established a simulation model of a 600 MW unit with LP cylinder near-zero output coupled with a thermal energy storage tank, and conducted simulation calculations and analysis. The results show that this coupled system can significantly broaden the thermoelectric feasible region of the unit and enhance its operational flexibility; furthermore, the deep peak shaving capacity of the unit after retrofitting is improved by 122.38 MW compared with that before retrofitting.

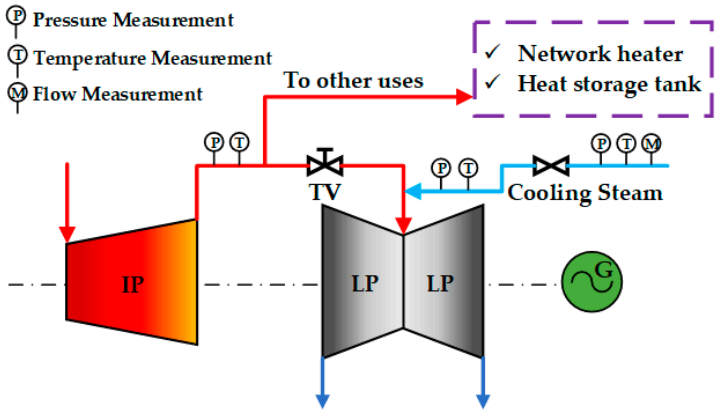


Figure 8. Schematic diagram of the near-zero output for LP cylinder of steam turbine [54,55].

There remains considerable room for improvement and retrofitting of steam turbine systems. The introduction of advanced algorithms (such as fuzzy control, predictive control, etc.), improvement of steam flow characteristics, optimization of blade design, and addition of energy storage coordination modules are not only key directions for future research but also critical technologies to enhance the deep peak shaving and fast peak shaving capabilities of coal-fired power units.

2.3. Fast Startup and Shutdown Technology for Coal-Fired Power Units

The rapid startup and shutdown technology for coal-fired power units serves as a key supporting technology for the transformation of coal-fired power from a "baseload power source" to a "flexible peak-shaving power source". This technology can significantly reduce the time required for a unit to transition from shutdown to grid-connected power generation (or from full-load operation to shut down) by optimizing key aspects such as equipment configuration, control systems, and operational strategies.

Current research on unit startup and shutdown, both domestically and internationally, primarily focuses on the development and optimization of the automatic procedure startup/shutdown system (APS). A mature and comprehensive APS must possess the capability to quickly adapt to grid dispatching requirements and load responses. Meanwhile, it needs to achieve deep integration with the core thermal control system of the unit, so as to fulfill the core objectives of "accurate response to grid commands, stable and reliable equipment operation, and strict compliance with environmental standards". He [57] proposed an optimization method for startup/shutdown control suitable for the deep peak shaving operation of coal-fired power units in thermal power plants. This method further improves the control logic of peak shaving startup/shutdown by adding power output constraints of the unit (including core parameters such as load ramp-up capability, power generation, and power output duration). A comparative experiment was carried out with a once-through pulverized coal-fired boiler as the research object. The results indicate that after adopting this optimization method, the average peak-valley difference rate of grid load reaches 22.2%, and the average daily load rate reaches 89.8%. This method not only reduces the peak-valley difference rate of grid load and increases the daily load rate but also effectively enhances the rationality of the startup/shutdown operation of coal-fired power units and their adaptability to grid peak shaving.

With the continuous increase in the proportion of grid-integrated renewable energy, frequent startup/shutdown will become a normal practice. However, the peak shaving depth achievable by optimized control systems is generally 25~40% of the rated load, making it difficult to achieve stable operation at low loads below 20% or near-zero loads (0~2%) [58]. CFB boilers possess advantages including a wide load adjustment range, large thermal inertia, and strong heat storage capacity. They also have the capabilities of banked fire and oil-free banked fire startup [59]. Theoretically, CFB boilers feature a peak shaving capability covering the 0~100% load range [60]. The typical CFB boiler structure and the principle of its banked-fire heat storage for peak-shaving are shown in Figure 9 [61,62]. Song et al. [63] conducted an experimental study on banked fire thermal standby and rapid startup/shutdown, with a 350 MW supercritical CFB power unit as the research object. The total banked fire duration in this experiment reached 108 min, during which all operating parameters of the unit remained stable. Successful oil-free fire revival was achieved in one attempt, and the unit enabled rapid startup, ramping up to 34 MW in approximately 6 min. The research results confirm that supercritical CFB coal-fired power units possess rapid startup and shutdown capabilities. Dong et al. [64] conducted a banked fire peak shaving experiment and optimized the control strategy, with a 350 MW supercritical CFB boiler unit as the research object. The experimental results show that after optimization, the supercritical CFB unit can achieve banked fire peak shaving at a unit load of 5~8 MW for 85 min. This confirms the feasibility of hour-level banked fire peak shaving for supercritical CFB units and can provide a reference for the engineering practice of similar units.

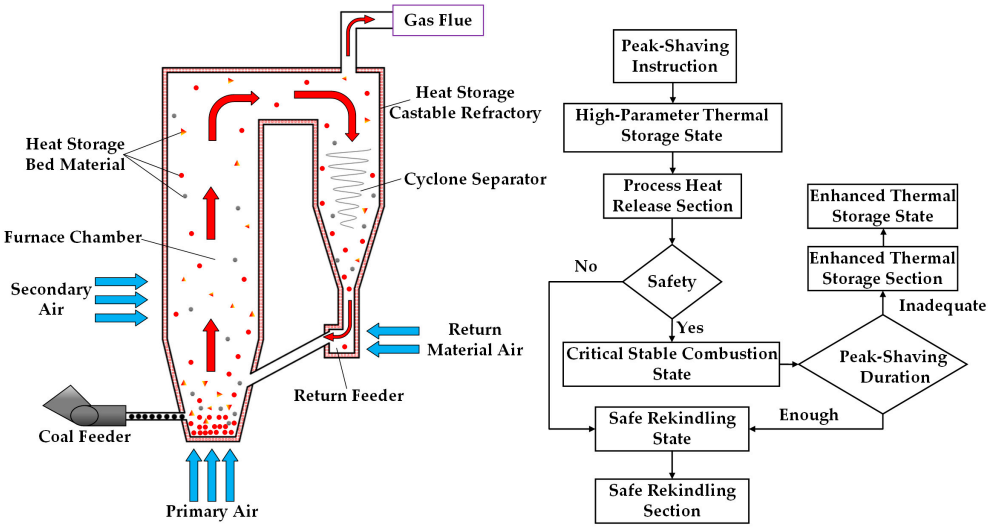


Figure 9. The typical CFB structure and principle of its banked-fire heat storage for peak-shaving [61,62]. (The red arrows in the figure indicate the flow direction of the fuel and the bed material.)

2.4. Economic Analysis of Flexibility Transformation for Coal-Fired Power Plants

In the context of high shares of renewable energy integrated into the power grid, the economic evaluation of flexibility retrofitting for coal-fired power units has gradually shifted from the traditional analysis based on "unit electricity cost" towards a comprehensive techno-economic assessment framework centered on operating scenarios and diversified revenue streams. Flexibility retrofitting does not necessarily increase the annual electricity generation of a unit; instead, its economic value is primarily reflected in enhanced system regulation capability arising from improved operational boundaries, such as reduced minimum stable output, increased ramping rates, and shortened start-up and shut-down times. Accordingly, on the revenue side, in addition to conventional electricity sales revenues, compensation from ancillary services—including peak shaving, frequency regulation, reserves, and capacity mechanisms—should also be taken into account. On the cost side, a systematic consideration is required of efficiency losses at low load, increased coal consumption, fuel use during start-up and shut-down, operation and maintenance expenses, lifetime degradation costs, and capital expenditures for equipment retrofitting. Taken together, the economic indicators adopted in current studies include net present value (NPV), internal rate of return (IRR), and investment payback period (IPP). Significant differences in net present value have been observed among different flexibility retrofit options, and local electricity price levels constitute a key factor influencing economic performance. Fu et al. [65] conducted an economic assessment of various retrofit schemes based on a typical 300 MW subcritical boiler and found that the maximum difference in net present value among the schemes reached CNY 36.2 million; an increase in electricity price of CNY 0.05 kWh^{-1} raised the net present value by CNY 15.35 million, and the highest IRR among the schemes was 36.12%, demonstrating that the implementation of an optimal retrofit option can yield substantial economic benefits. Meng et al. [66] performed an economic analysis of a coupled wind–solar–coal power plant in Liaoning Province, China, and found that increases in coal prices reduce the net peak-regulation revenue of the plant, which may even become negative.

The rapid peak shaving technology for coal-fired power in China is still in its initial stage, with the maximum load ramp-up rate of units being approximately 2% per minute [67]. Currently, the proportion of power generation from renewable energy sources, mainly wind and solar power, is increasing rapidly year by year. This makes

the market demand for rapid startup/shutdown of coal-fired power units increasingly urgent—particularly the demand for coal-fired power generating units with dual capabilities of long-duration banked fire thermal standby and rapid startup/shutdown will be more pressing. However, there is currently no effective technology to support long-duration banked fire thermal standby and rapid startup/shutdown of coal-fired power units, especially for pulverized coal-fired utility boilers. Therefore, there is an urgent need to carry out R&D and achieve breakthroughs in relevant technologies.

3. State of Development of Energy Storage Technologies

The global energy mix is undergoing a profound transformation, and the proportion of electricity generation from renewable energy sources—with wind power and photovoltaic power as representatives—continues to rise. Energy storage technologies can effectively mitigate the volatility of renewable energy power output, enhance the power grid's accommodation capacity for high-proportion renewable energy, and simultaneously improve the peak-shaving capability of CFPP, thereby facilitating CFPP to realize the transition from "base-load power sources" to "flexible peak-shaving power sources". Thus, the coupling of energy storage technologies with CFPP has become one of the key approaches to enhancing grid flexibility and ensuring the safe and stable operation of power systems.

Traditional energy storage technologies encompass a wide range of types, and in their coupling applications with new energy sources, they can be categorized into physical energy storage, electrochemical energy storage, and thermal energy storage, among others, based on energy storage principles.

3.1. Physical Energy Storage

Physical energy storage is currently the most widely used energy storage method in China, including compressed air energy storage, gravitational energy storage, flywheel energy storage, and so on. Physical energy storage methods generally feature a long lifespan and large capacity, and are applied in many large-scale engineering projects.

3.1.1. Compressed Air Energy Storage

Traditional compressed air energy storage (CAES) is a large-scale energy storage technology that stores energy by compressing air and releases high-pressure air to drive generators for power generation when needed, whose working principle is illustrated in Figure 10. Geweda et al. [68] analysed the progress, design standards, and improvement strategies of CAES technology, concluding that it features high energy capacity, high power output, long service life, and cost-effectiveness, with strong competitiveness and substantial potential for large-scale deployment.

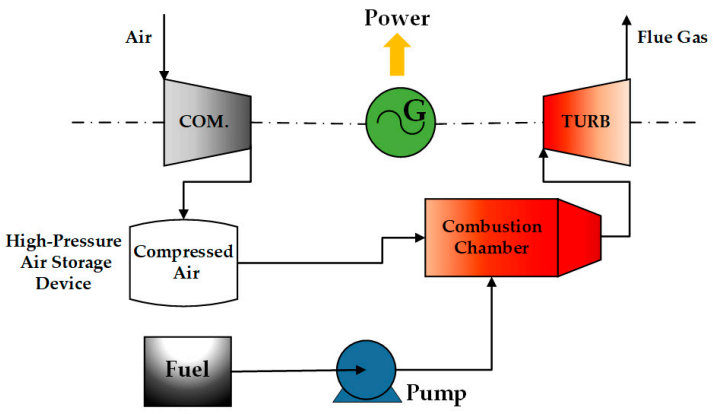


Figure 10. CAES working principle schematic diagram. (COM. is compressor; TURB is turbine).

With the development of novel adiabatic technologies, thermal storage system optimization technologies, and underground gas storage reservoirs, CAES is expected to become a key supporting technology for large-scale grid integration of renewable energy [69]. The CAES system can effectively reduce the investment cost of its own heat storage segment, while broadening the peak regulation margin of CFPP [70]. Existing studies have coupled the CAES system with CFPP and conducted feasibility and techno-economic analyses [71]. Wang et al. [72] proposed a CAES system coupled with coal-fired power units, whose working principle is illustrated in Figure 11. The results showed that through the rational coupling of the CAES system with the thermal cycles of coal-fired power units, the system efficiency can be increased by 5 percentage points.

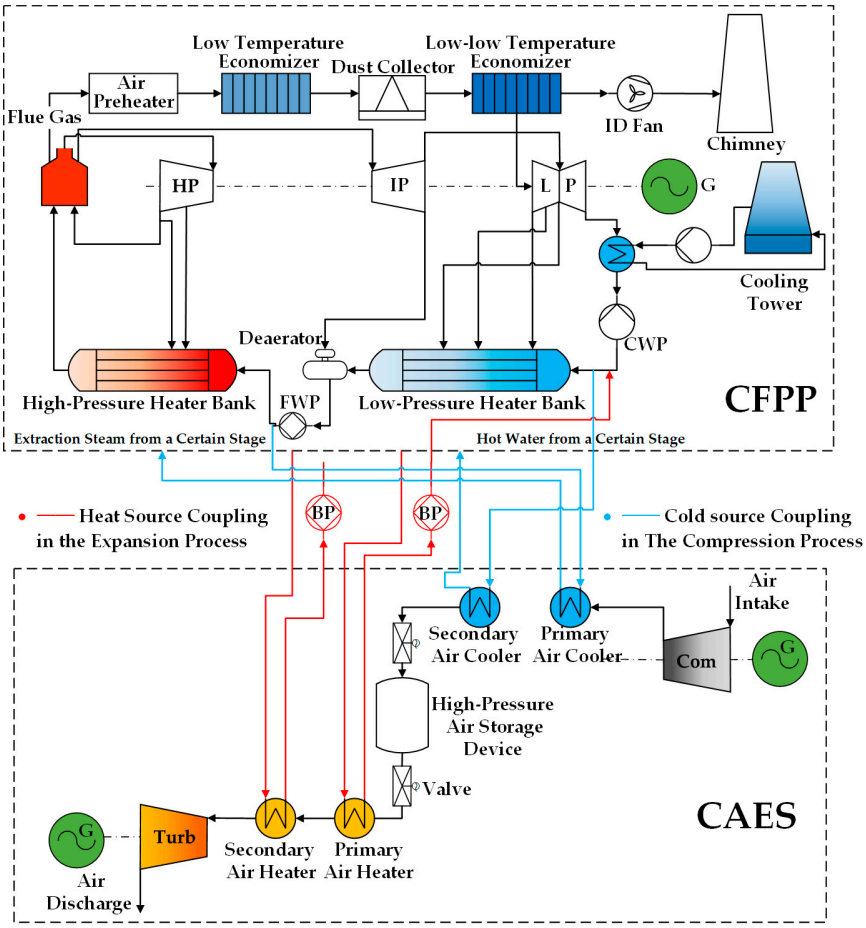


Figure 11. Schematic diagram of the operating principle of a CAES system coupled with a CFPP [72].

Besides air, CO_2 can also serve as the working fluid in energy storage systems. Moreover, CO_2 is easier to reach the critical state and has a higher energy density. Hou et al. [73] proposed a novel liquid CO_2 energy storage system that can be integrated with coal-fired power units. As shown in Figure 12, during the energy storage stage, this system directly utilizes the condensation water of CFPP to recover the compression heat, and can achieve an electricity storage efficiency of 55.04%, representing an increase of 8.04% compared with the pre-integration level.

3.1.2. Flywheel Energy Storage

Flywheel Energy Storage Systems (FESS) store energy by converting electrical energy into the kinetic energy of a high-speed rotating flywheel, and reversibly convert the flywheel's kinetic energy back into electrical energy when needed. FESS can respond to

grid frequency changes with a response speed at the millisecond level [74]; by rapidly charging and discharging to absorb or release energy, they mitigate frequency fluctuations in renewable energy output, thereby enhancing grid stability.

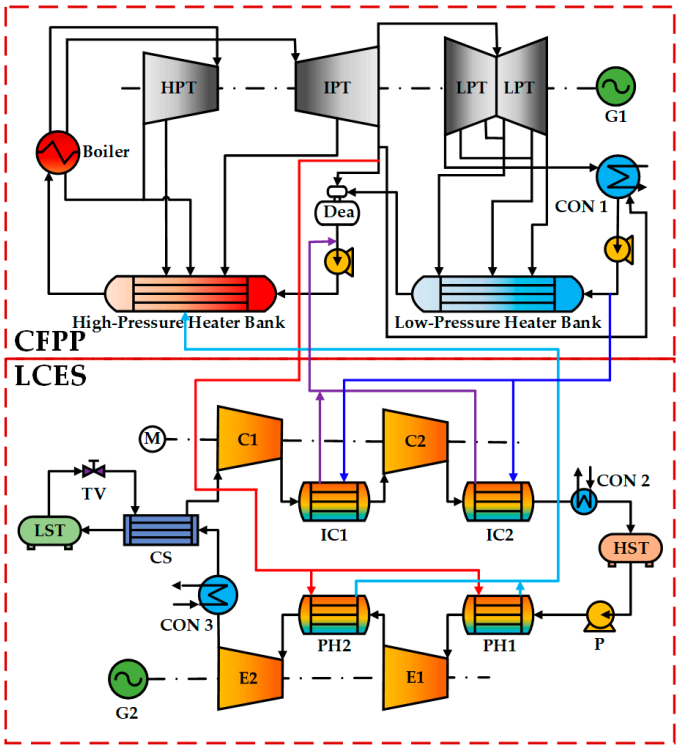


Figure 12. Schematic diagram of the operating principle of a LCES system coupled with a CFPP [73].

Currently, there are relatively few experimental studies on the coupling of FESS with coal-fired power units, with most being simulation studies.

Song et al. [74] established a linear model for frequency regulation of coal-fired units assisted by flywheel energy storage and conducted simulation experiments. The simulation results show that adding a flywheel with a capacity of 2.5% can reduce the maximum frequency deviation by 22% and the maximum power deviation by 21% under step disturbances. This verifies the possibility of using FESS to assist coal-fired units in frequency regulation under large-scale renewable energy grid integration conditions. Elbouchikhi et al. [75] developed a scaled-down experimental setup for a domestic flywheel energy storage system. Based on this setup, case studies and experiments were conducted, and the results demonstrated the potential of flywheel energy storage for grid-connected applications.

Although FESS have significant potential in peak shaving for coal-fired power units, they still face challenges such as relatively high initial investment costs, inflexible configuration and operational strategies, and short storage durations. To enable the widespread application of flywheel energy storage, it is necessary to further optimize the configuration and operational strategies, develop efficient and coordinated control algorithms, and for long-duration energy storage needs, integrate with other energy storage technologies, such as battery storage.

3.2. Electrochemical Energy Storage

Electrochemical energy storage mainly refers to battery storage, which is characterized by fast response times and high energy density. In the coupling system of electrochemical energy storage and coal-fired power units, the common types of batteries include lithium-

ion batteries, redox flow batteries, lead-acid batteries, and solid-state sodium batteries. The structures and principles of these batteries are illustrated in Figure 13 [76–79].

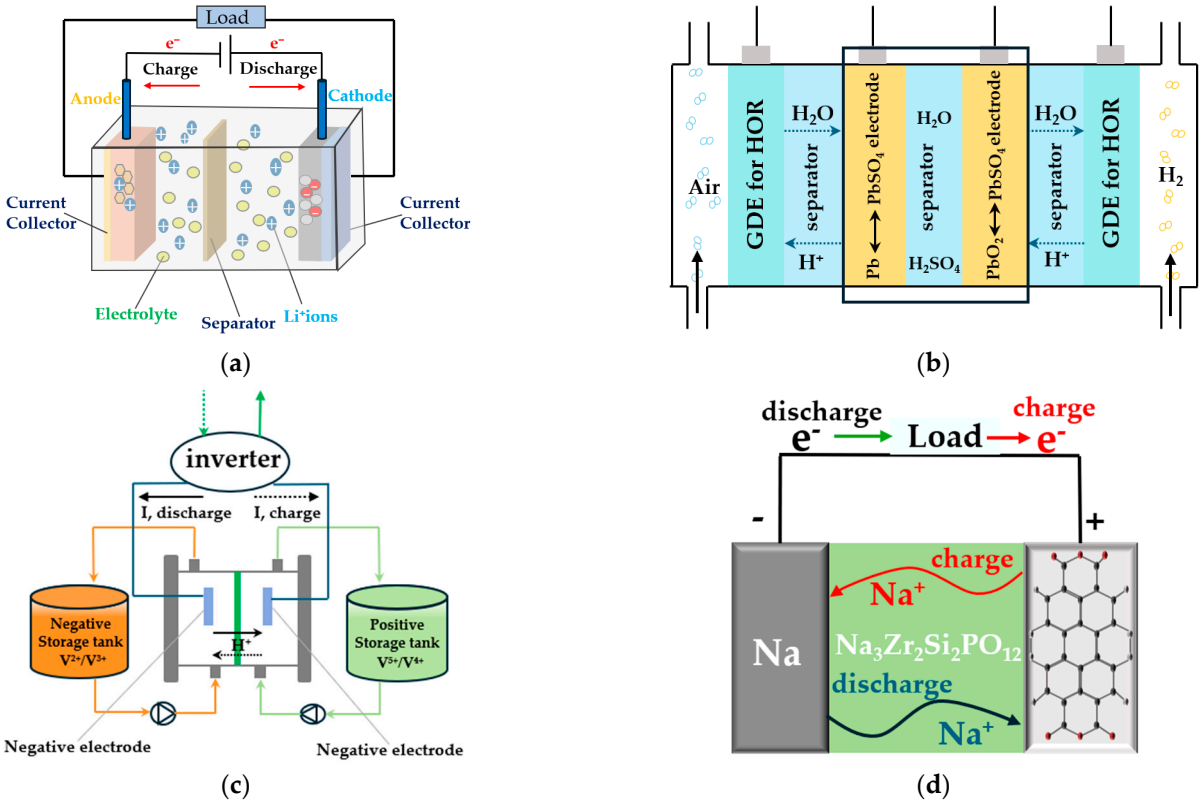


Figure 13. (**a**) Structure of the lithium-ion cell [76]; (**b**) Structure of the Pb acid battery [77]; (**c**) Structure of the vanadium redox flow battery [78]; (**d**) Structure of the solid-state sodium batteries [79].

3.2.1. Lithium-Ion Battery Energy Storage

Nowadays, lithium-ion batteries are one of the most widely used electrochemical energy storage technologies, offering high energy density and long cycle life. Compared to other energy storage technologies, lithium-ion batteries are more suited for small-scale applications and do not rely on specific geographical conditions (such as remote areas), allowing for more frequent usage [76]. In power systems, they perform excellently in frequency and load regulation [80]. However, the high cost of lithium-ion batteries limits the large-scale application of lithium-ion battery energy storage.

A large number of studies have proposed solutions for optimizing the cost structure of lithium-ion battery energy storage, with the aim of advancing its commercialization process [81]. Furthermore, future development directions include the development of safer, more efficient, and environmentally friendly lithium-ion batteries, as well as the exploration of new battery technologies, such as solid-state batteries, sodium-ion batteries, and potassium-ion batteries [82–85].

3.2.2. Redox Flow Battery Energy Storage

A flow battery is an electrochemical energy storage device that achieves the conversion between electrical energy and chemical energy through the redox reactions of active substances in the positive and negative electrode electrolytes. The electrolyte is stored in external tanks and circulates through the electrochemical stack via pumps, where redox reactions occur on the surfaces of the electrodes, thus enabling the battery's charging and discharging process.

The power of a flow battery is determined by the size of the electrochemical stack, while the capacity depends on the size of the electrolyte storage tank and the electrolyte concentration. This allows for flexible configuration of power and capacity based on actual demand [86]. It also offers high safety, long lifespan, high energy efficiency, and environmental friendliness, among other advantages [87,88].

Common types of flow batteries include vanadium redox flow batteries, iron-based flow batteries, zinc–bromine flow batteries, and organic flow batteries. Ouyang et al. [89], based on the coupling of a vanadium redox flow battery with a rural microgrid system, proposed a predictive control approach to enhance the efficiency of flow batteries and conducted simulation analyses. The results indicated that the adoption of predictive control can significantly improve the performance of flow batteries, with the overall peak-shaving efficiency reaching 84%.

The high cost has hindered the large-scale development of flow batteries, and compared with other types of batteries, flow batteries also suffer from low energy density. At the same time, there remains considerable room for improvement in the performance of both the electrolyte and the electrochemical stack of flow batteries [90].

3.3. Thermal Energy Storage

Thermal energy storage technology, by storing heat and releasing it when required, can enhance energy utilization efficiency, facilitate the integration of renewable energy, and improve grid flexibility [91], playing a crucial role in the coupling of coal-fired power generation and renewable energy.

According to the principle of heat storage, thermal energy storage can be classified into sensible heat storage, latent heat storage, and thermochemical heat storage. Thermal energy storage designed to support the large-scale integration of renewable energy into the grid needs to feature large storage capacity and high operating temperatures. Common thermal energy storage media include molten salts, solid particles, and heat transfer oils.

3.3.1. Molten Salt Thermal Energy Storage

Molten salt thermal energy storage systems employ molten salts as the storage medium, characterized by high thermal storage density and a wide operating temperature range [92]. In the field of renewable energy, the application of molten salt thermal energy storage is primarily concentrated in concentrated solar power [93], with its operating principle illustrated in Figure 14.

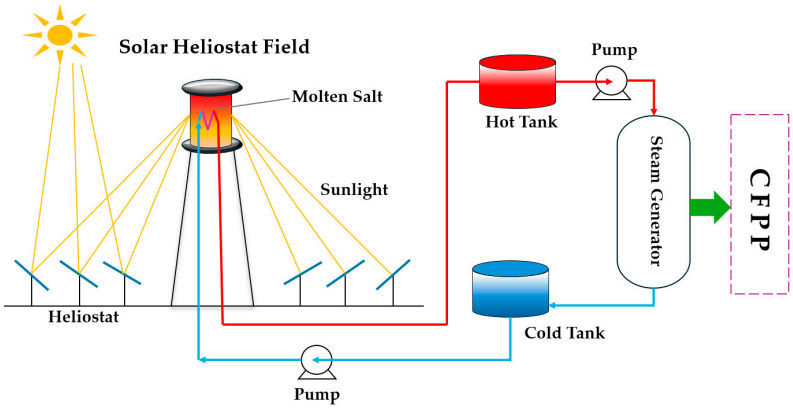


Figure 14. Concentrated solar power coupled with CFPP integrated MSTES system schematic diagram [93].

Molten salt thermal energy storage systems can absorb thermal mismatches between the boiler and the steam turbine, and its integration into coal-fired power plants holds the

potential to decouple the operation of the boiler and the turbine [94]. Liu et al. [95] proposed three molten salt thermal storage configurations—series, parallel, and hybrid. Based on simulation studies of a 600 MW supercritical coal-fired unit, the results demonstrated that integrating a molten salt thermal energy storage system can broaden the operational flexibility of coal-fired units. Without reducing the boiler's thermal load, the minimum unit load can be decreased from 30% to 19.02% of the rated capacity.

Large-scale energy storage imposes higher requirements on energy conversion and storage efficiency, which implies that the storage medium must operate under higher temperature conditions. However, molten salt undergoes decomposition under high-temperature conditions and cannot operate reliably above 800 °C. In addition, molten salt thermal storage faces issues such as low-temperature solidification, high-temperature corrosion, and pipeline blockage, which require further optimization and improvement.

3.3.2. Other Thermal Energy Storage Methods

Under high-temperature operating conditions, solid particle thermal storage media exhibit greater application advantages compared with conventional options such as molten salts, due to their lower cost, higher storage temperatures, and superior physicochemical properties. Since 2020, they have gradually emerged as a prominent research focus in the field of energy storage [96,97]. Nevertheless, experimental investigations into the integration of solid particle thermal storage with coal-fired power units remain relatively scarce.

In small-scale thermal storage systems, phase change materials and thermochemical materials also serve as effective storage media. Examples include paraffin wax and salt hydrates. Such materials typically exhibit higher energy densities, making them particularly advantageous for enhancing the efficiency and compactness of thermal energy storage applications.

The advantages of latent heat storage lie in its high energy density and large storage capacity; however, its poor thermal conductivity often necessitates the adoption of heat transfer enhancement measures [98,99].

Thermochemical energy storage (TCES) relies on reversible chemical reactions to store or release heat. For example, energy can be stored through the decomposition of $CaCO_3$ into CaO and CO_2, and subsequently released through the reverse reaction in which CaO and CO_2 recombine to form $CaCO_3$. TCES has the advantage of extremely high energy density, enabling long-term energy storage and even cross-seasonal energy storage. However, it currently remains in the laboratory stage and lacks specific industrial demonstration applications.

3.4. Comparative Analysis and Summary of Energy Storage Technologies

With the rapid expansion of renewable power generation, the demand for energy storage is increasingly characterised by larger scale and greater flexibility. To address the diverse requirements across different application scenarios, it is essential to select and configure appropriate types of energy storage technologies. Therefore, a comparative analysis of energy storage technologies is necessary. A comparison of several commonly applied energy storage technologies is presented in Table 2.

Table 2. Comparative table of selected energy storage technologies.

Energy Storage Technologies	Key Characteristics	Applications
CAES	High compatibility, enabling the reuse of existing infrastructure; favourable safety performance and environmental sustainability; strong dependence on geographical conditions; high upfront investment and long payback.	300 MW Advanced CAES National Demonstration Power Station, Institute of Engineering Thermophysics (CAS) [100] 660 MW Man-Made Cavern-Type CAES Power Station Demonstration Project, Dunhuang, Jiuquan, Gansu [101]
FESS	Well-suited for high-frequency regulation, with a long cycle life; without chemical reactions, high safety and zero pollutant emissions; extremely short storage duration, making it unsuitable for long-duration peak shaving.	Maglev FESS project of Shandong Penglai Company [102]
RFBES	Long cycle life and slow capacity degradation, making it well-suited for long-duration peak shaving; power and capacity can be independently configured; wide operating temperature range, enabling adaptation to the complex conditions of power plants.	Megawatt-scale iron–chromium flow battery energy storage demonstration project [103] Grid-Forming Vanadium RFBES Project [104]
LIBES	Fast response, capable of meeting rapid peak-shaving and frequency regulation requirements; high energy density with a high degree of system integration, resulting in a small spatial footprint; technologically mature, supported by a well-established industrial supply chain, with continuously declining costs.	18 MW/6.672 MWh lithium-titanate battery energy storage system [105]
MSTES	Highly compatible with conventional coal-fired thermal systems, it can be directly integrated with boilers and steam turbines to achieve boiler–turbine decoupling, thereby enhancing peak-shaving depth to below 20%; large thermal storage capacity, making it suitable for long-duration energy storage systems; molten salts are highly corrosive and relatively expensive.	The “Coal-Fired Power + Molten Salt” Energy Storage Project [106]
SPTES	High storage temperature and strong physicochemical stability, making it suitable for large-scale, long-duration energy storage systems; low material cost of storage media; how-ever, limited heat transfer efficiency and low techno-logical maturity.	MW-scale High-Temperature Solid Particle Heat Storage Pilot-Scale Test [107]

3.5. Economic Analysis of Coupled Energy Storage Technology for Coal-Fired Power Plants

The economic analysis of integrating energy storage modules into coal-fired power systems typically adopts a "coal unit–energy storage co-operation" framework, in which the compositions of the revenue and cost sides are similar to those of coal unit flexibility retrofitting, while particular attention must be paid to differences among storage technologies in terms of response speed, storage duration, and cost structures. Bai et al. [108] integrated CAES with a combustible solid waste power plant and conducted efficiency and economic analyses, showing that the integrated system achieved an electrical efficiency of 85.70%, a dynamic payback period of 3.79 years, and a net present value of USD 1.679 million, indicating favorable economic performance. Grimaldi et al. [109] comprehensively evaluated the techno-economic feasibility of coupling BESS with wind power plants for grid integration, comparing BESS power and capacity at different scales, and found that integrating 1 h and 2 h batteries into wind power systems yields the highest economic benefits, with a maximum net present value of EUR 152 thousand, demonstrating the critical role of energy storage in the profitability of renewable energy projects. Liu et al. [95] proposed three coal-fired power plant–molten salt thermal energy storage integrated systems based on different molten salt heating configurations and performed an economic assessment, showing that the minimum load of the integrated system could be reduced to 19.02%, while the series, parallel, and hybrid configurations achieved net present values of USD 37.72 million, USD 16.56 million, and USD 19.15 million, respectively. Overall, energy storage modules exhibit strong economic competitiveness in coal–renewable coupled power systems.

Energy storage technologies still face numerous challenges in assisting coal-fired power coupling with renewable energy generation for grid integration. On the one hand, large-scale deployment places higher demands on the energy density and operational safety of storage systems; on the other hand, the risk of secondary hazards triggered by storage system configurations during disasters has yet to be effectively mitigated. At present, the maturity, economic viability, and system reliability of various storage technologies remain insufficient to support the requirements of ultra-large-scale strategic energy reserves. Nevertheless, the rapid expansion of renewable energy will inevitably continue to drive innovation and iteration in storage technologies, with the aim of overcoming the key technological bottlenecks associated with large-scale energy storage.

4. Current Status of Co-Firing Technologies with Zero-Carbon Fuels and Coal

Zero-carbon fuels refer to fuels that achieve zero or near-zero greenhouse gas emissions during their production or utilization, including hydrogen, ammonia, and certain types of biomass. Co-firing zero-carbon fuels with coal can enhance the environmental performance of power generation. The gradual introduction of zero-carbon fuels into conventional coal-fired power generation can reduce dependence on fossil fuels while maintaining the stability of the energy system. This paper focuses on their role in reducing carbon emissions, improving the operational flexibility of coal-fired units, and facilitating the integration of renewable energy. Common zero-carbon fuels for coal co-firing include biomass, ammonia, and hydrogen, among others.

4.1. Biomass–Coal Co-Firing Technology

Biomass–coal co-firing technology refers to the process of blending biomass fuels (such as wood chips, straw, and rice husks) with coal in specified proportions, and combusting them together in coal-fired boilers to reduce carbon emissions and enhance energy efficiency.

Since 2015, the production of biomass briquette fuel in China has been increasing year by year, as shown in the Figure 15 [110].

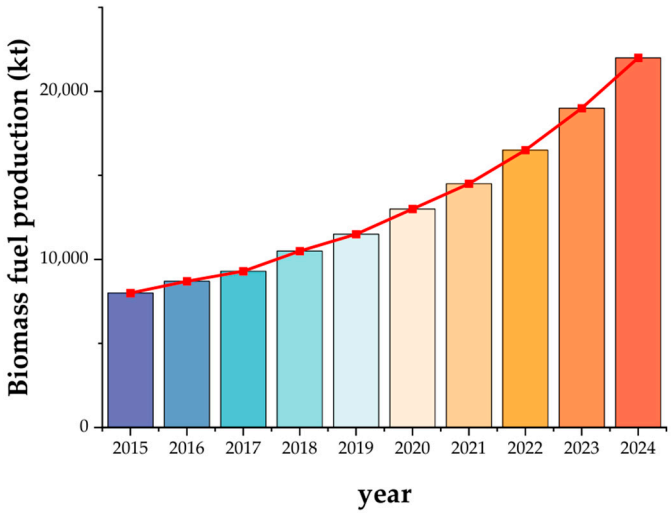


Figure 15. Chart of biomass briquette fuel production changes in China from 2015 to 2024 [110].

4.1.1. Impact of Biomass Type

Different types of biomass, due to variations in moisture content, compositional characteristics, and combustion properties, exert distinct impacts on co-firing performance, particularly in terms of combustion efficiency, slagging and corrosion, and pollutant emissions.

Extensive research has been conducted in China on the co-firing of different types of biomass with coal. Liu et al. [111] simulated a 660 MW supercritical opposed-firing coal boiler co-firing five types of biomass (wheat, maize, rice, giant reed, and wood) at blending ratios ranging from 0~50%, and compared the results with experimental data from a direct-fired boiler unit. The study found that co-firing wheat straw, maize straw, and giant reed increased flue gas volume and reduced theoretical combustion temperature, whereas co-firing rice and wood exhibited the opposite trend. The findings indicated that giant reed is better suited for high-sulfur coal boilers prone to severe high-temperature corrosion, while rice and wood are more appropriate for boilers firing lean coal or anthracite with significant unburned carbon losses. Zhao et al. [112] found that the impact of biomass co-firing on boiler systems varies significantly with biomass type. Compared with rice straw and other crop residues, wood chips exert a smaller effect on slagging in coal-fired power generation systems. Moreover, the acceptable biomass blending ratio differs among boiler configurations.

4.1.2. Direct Co-Firing

Direct co-firing refers to the technology of blending biomass fuels with coal in specified proportions and combusting them together directly in coal-fired boilers, as shown in Figure 16. Direct co-firing requires minimal equipment retrofitting, offers high power generation efficiency, and involves relatively low initial investment, making it the predominant co-firing approach in China.

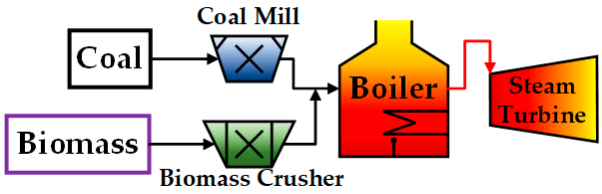


Figure 16. Schematic diagram of direct co-firing of biomass and coal.

In order to more effectively achieve the goals of "carbon reduction, cost reduction, and efficiency improvement" during the energy transition, scientists worldwide have been striving to increase the proportion of biomass co-firing with coal. Jiang et al. [113], through comparative analysis of the combustion characteristics of coal-fired boilers under pure coal firing and coal–biomass co-firing conditions, found that biomass co-firing can significantly reduce CO_2 and SO_2 emissions, with a 15% biomass blending ratio identified as the most suitable for practical engineering applications. A study has shown that when the co-firing ratio exceeds 15%, combustion characteristics changes markedly, as higher biomass proportions may lead to unstable combustion, flame oscillations, or deflagration, thereby increasing the operational risks of the combustion system.

In general, high shares of biomass co-firing may result in reduced combustion stability and efficiency of boilers, increased risks of slagging and corrosion, and fluctuations in pollutant emissions. To date, several demonstration projects have been completed in China, with the maximum co-firing ratio (by mass) reaching 25%. At the Caojing Power Plant of Shanghai Electric, a 1000 MW unit carried out a large-scale co-milling and co-firing test with energy crops, blending super giant reed pellets (dry-based calorific value: 4500 Cal/kg) uniformly with coal, pulverizing them in coal mills, and feeding the mixture into the boiler for combustion. The biomass share reached 25%, resulting in an annual CO_2 reduction of approximately 440,000 tonnes [114]. At the Shengli Power Plant of China Energy's Guodian Power, the country's first large-scale "coal-fired unit co-firing with cattle manure" was successfully demonstrated, where cattle manure was co-combusted with lignite at a blending ratio of 15% [115].

4.1.3. Biomass Gas Co-Firing (Indirect Co-Firing)

Biomass gas co-firing refers to the process in which biomass fuels are converted into combustible gas through gasification technology, and the resulting syngas is subsequently co-fired with coal, as shown in Figure 17. This approach can mitigate ash deposition and slagging in coal-fired boiler units, with the theoretical co-firing ratio increasing to as much as 30% [116]. However, it requires the installation of additional gasifiers, thereby raising the costs associated with technical retrofitting.

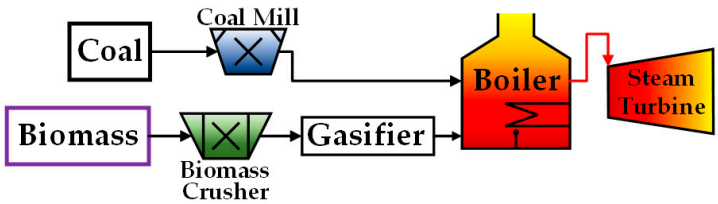


Figure 17. Schematic diagram of indirect co-firing of biomass and coal.

Fan et al. [117] have proposed a multi-stage energy utilization system that utilizes flue gas from cement kilns for drying sewage sludge and biomass, followed by the adoption of co-gasification technology to produce syngas, which is then used for power generation through combustion. Simulation results indicate that the energy efficiency and exergy efficiency of this system are 44.03% and 47.48%, respectively. Chen [118] proposed a

coupled biomass air–steam gasification and coal-fired boiler system model based on waste heat and water recovery, and conducted simulation analyses. The co-firing ratio of the coupled system ranged from approximately 2% to 43%. The simulation results showed that as the co-firing ratio increased, boiler thermal efficiency gradually decreased from 92.94%, while the maximum reduction in flue gas pollutants was 43.38% for CO_2, 28.27% for SO_x, and 50.47% for NO_x. Han [119], based on a 660 MWe coal-fired boiler and a 30 t/h biomass gasifier, conducted a systematic study on the co-firing characteristics and pollutant emissions of syngas derived from pinewood, wood chips, and sludge. The results showed that wood-chip-derived gas achieved the most effective NO_x reduction, while pinewood gas yielded the highest system efficiency. Moreover, the biomass gas co-firing ratio was strongly influenced by boiler load, with lower loads allowing for higher biomass gas shares.

Biomass can also be directly combusted to produce steam, which is subsequently coupled with coal-fired boilers on the steam side, as shown in Figure 18. The steam-side coupling of biomass enables the decoupling from the intrinsic physicochemical constraints of biomass fuels, thereby offering strong adaptability. However, this approach requires the installation of an additional biomass boiler and supporting auxiliary systems, while the efficiency of biomass boilers is significantly lower than that of coal-fired units, which limits its practical application.

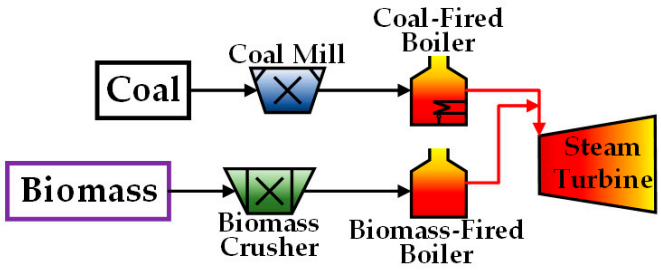


Figure 18. Schematic diagram of the steam-side coupling principle between biomass and coal.

4.1.4. Other Influencing Factors

Biomass co-firing with coal can effectively reduce carbon emissions; however, in practical applications, the evaluation criteria should not be limited solely to carbon abatement outcomes. Al-Qayim et al. [120] conducted a techno-economic assessment of a UK power plant applying white wood pellet co-firing with coal in combination with carbon capture and storage (CCS) technology. The study revealed that although co-firing white wood pellets could reduce CO_2 emissions by approximately 3 million tonnes annually, it also adversely affected both power generation efficiency and generation costs. Similarly, Xie et al. [121] examined the integration of biomass co-firing with CCS in coal-fired power plant decarbonization, demonstrating significant mitigation potential while also highlighting the associated risk of environmental burden shifting. Collectively, these findings indicate that before large-scale deployment of such technologies, it is essential to undertake comprehensive multi-dimensional assessments—encompassing carbon mitigation, economic viability, and environmental impacts—in order to achieve an integrated optimum.

In summary, biomass, as the only carbon-containing renewable energy currently, can partially substitute coal through co-firing, thereby enabling low-cost carbon mitigation and emission reduction. However, further research is required to increase the co-firing ratio and to ensure stable combustion performance.

4.2. Ammonia-Coal Co-Firing Technology

Ammonia is a carbon-free, hydrogen-rich fuel with substantial potential for energy applications. Ammonia–coal co-firing technology has attracted widespread global atten-

tion in the context of energy transition research, with several countries setting specific development targets. China has announced plans to reduce the average carbon emission intensity of coal-fired power units by around 50% by 2027, requiring retrofitted plants to achieve a co-firing capacity of more than 10% green ammonia [122]. Japan aims to achieve approximately 20% ammonia co-firing in coal-fired units by around 2030, while expanding nationwide deployment and advancing demonstrations of high-ratio co-firing and dedicated combustion technologies [123]. South Korea has proposed that by around 2030, more than half of its coal-fired units will operate with 20% ammonia co-firing [124].

Ammonia–coal co-firing technology also faces several challenges:

- The combustion rate of ammonia is extremely slow, making newly introduced ammonia difficult to ignite;
- The vaporization of liquid ammonia absorbs a large amount of heat, leading to a sharp drop in temperature, which further increases the difficulty of combustion;
- The high nitrogen content of ammonia increases the risk of NO_x emissions when co-fired with coal.

4.2.1. Combustion Characteristics of Ammonia and Coal Co-Firing

The combustion characteristics of ammonia and coal differ considerably, and their co-firing process may lead to issues of combustion instability. Moreover, varying ammonia co-firing ratios can also significantly influence the morphology and stability of the combustion flame.

Liu et al. [125] developed a cylindrical combustion chamber model to simulate the effects of 0~50% ammonia co-firing ratios and air injection positions on flame structure, NO_x formation, and combustion efficiency. The simulations indicated that with central injection of 20~30% ammonia, the flame morphology shifted from a swirling to a slender shape, and the NO concentration decreased to 11.2 mg/Nm^3. At a co-firing ratio of 50%, a "candle-type" flame developed, accompanied by a marked increase in NO emissions. Lee et al. [126] investigated ammonia–coal co-firing and found that the flame propagation speed of ammonia combustion is influenced by ambient conditions and the type of co-fired coal (high/low fuel ratio). The results indicated that low fuel ratio coal is more conducive to stable combustion. Hadi et al. [127] investigated the influence of coal fuel ratio on the turbulent flame speed in ammonia and coal co-firing. Experimental results demonstrated that the co-firing flame speed with bituminous coal was three times that of pure coal and twice that of pure ammonia, whereas the flame speed of high fuel ratio coal blends was lower than that of pure ammonia. Zhang et al. [128] investigated the flame stability and emission characteristics of ammonia combustion in a gas turbine combustor and found that employing auxiliary measures such as elevated pressure conditions and plasma-assisted ignition can enhance flame stability while reducing NO emissions.

4.2.2. NO_x Emission Characteristics of Ammonia–Coal Co-Firing

The nitrogen-containing property of ammonia makes it generate more NO_x during combustion, especially under high blending ratios, where it tends to exceed emission standards. The main formation and conversion pathway of NO_x during ammonia-coal co-fired are illustrated in Figure 19 [129–132]. Currently, commonly applied strategies to mitigate NO_x generation include staged combustion, optimization of co-firing ratios, SCR, and adjustment of overfire air nozzle positions, among others.

Zhang et al. [133] conducted industrial-scale tests in a 40 MW_{th} coal-fired boiler to investigate the combustion behaviour and NO_x emission characteristics under high ammonia co-firing ratios (0~25%). The results demonstrated that stable combustion could be maintained at these co-firing ratios, while NO_x emissions could be controlled to levels

below those of pure coal combustion through air-staging technology. This study provides experimental evidence and operational guidance for the application of ammonia co-firing technology in large-scale coal-fired boilers. Wang et al. [134] examined the impact of partial ammonia co-firing on the operational performance of a 600 MW supercritical pulverized coal boiler. The results indicated that at a 10% co-firing ratio, CO concentration in the combustion zone decreased, while NO_x generation increased, leading to an approximately 6.3% rise in NO_x concentration at the furnace outlet. As the co-firing ratio increased (0~40%), NO_x concentration at the furnace outlet first rose and then declined, peaking at 10% co-firing. Moreover, excessively high ammonia co-firing ratios resulted in ammonia slip.

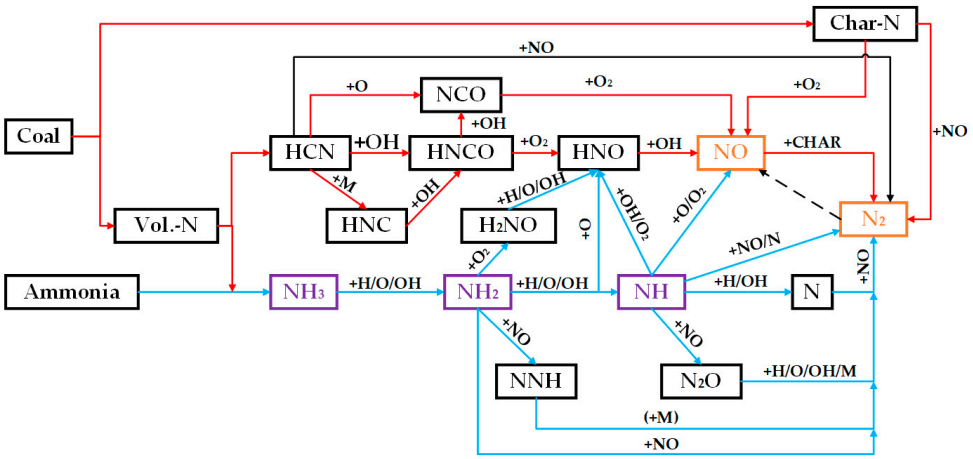


Figure 19. The main formation and conversion pathway of NO_x during ammonia-coal co-fired [129–132].

Tan et al. [135] investigated the effects of ammonia injection method, co-firing ratio, and reaction temperature on flue gas composition and combustion efficiency, finding that staged combustion can reduce the formation of char-NO_x and fuel (NH_3)-NO_x. When the co-firing ratio was ≤30%, NO_x emissions were comparable to those of coal-only combustion, confirming the potential of ammonia as a substitute fuel for CO_2 reduction. Wang et al. [136] conducted ammonia–coal co-firing experiments using bituminous coal in a 45kW staged-combustion furnace, applying an overall air-staging strategy. The experimental results showed that the position of the overfire air nozzles had a significant impact on the co-firing products: the further the nozzles were from the burner outlet, the lower the NO concentration. However, when the distance was excessively large, the NO reduction efficiency exhibited limited improvement, and may even exert a negative impact on combustion efficiency.

Chen et al. [137] employed a combined approach of experimental testing and density functional theory to systematically investigate the heterogeneous NO reduction mechanisms in the high-temperature reducing zone under coal–ammonia co-firing conditions. The findings revealed that ammonia co-firing enhanced NO reduction in the reducing zone and exhibited a synergistic effect with char in promoting heterogeneous NO reduction, thereby advancing the understanding of nitrogen transformation pathways in coal–ammonia co-combustion.

Collectively, these studies provide concrete and feasible research insights into enabling synergistic reductions of CO_2 and NO_x through ammonia–coal co-firing technology.

4.2.3. Engineering Applications of Ammonia–Coal Co-Firing

At present, China has achieved the highest ammonia–coal co-firing ratio in engineering applications worldwide, reaching up to 35%, with pilot platforms capable of attaining 40%, while other countries typically operate at around 20%. The Energy Research Institute of the Hefei Comprehensive National Science Center successfully achieved stable operation with a 35% ammonia co-firing ratio in a 300 MW coal-fired unit at Waneng Tongling Power Company (Tongling, China) [138]. The Xi'an Thermal Power Research Institute of China Huaneng Group (Erdos, China) validated the combustion stability of up to 40% ammonia co-firing on a 4 MW pilot platform, with NO_x emissions and combustion efficiency comparable to those of pure coal firing [139]. Japan's JERA (Tokyo, Japan) successfully demonstrated stable combustion with a 20% ammonia co-firing ratio in Unit 4 of the 1000 MW Hekinan Power Plant [140].

In summary, ammonia–coal co-firing technology is still at a developmental stage, where approaches such as staged combustion, optimizing the coal–ammonia co-firing ratio, and coal–ammonia co-pyrolysis can enhance combustion stability and mitigate NO_x emissions. However, key technologies—including large-scale ammonia supply, clean ammonia combustion, and flexible operational strategies—remain to be advanced. The fundamental mechanisms of coal–ammonia dual-phase co-firing require further investigation, and there is still a lack of low-NO_x, full-flow stable combustion technologies [141].

4.3. Hydrogen-Coal Co-Firing Technology

Hydrogen, as a clean fuel with high energy density that can be produced directly via water electrolysis powered by renewable electricity, is gaining increasing prominence under the global energy transition and the targets of the Paris Agreement. With the advancement of carbon reduction targets, coal-fired power units are under mounting pressure to cut emissions, making the transition towards low-carbon operation an urgent necessity. Due to its high calorific value and rapid combustion rate, hydrogen co-firing with coal can enable boilers to respond more swiftly to load variations and support coal-fired unit stable combustion under low-load conditions. Building on these advantages, hydrogen–coal co-firing represents an emerging technology with substantial potential for future development.

Hydrogen–coal co-firing technology also faces a series of challenges:

- The large-scale deployment of hydrogen energy has not yet been realized, and the costs associated with its transportation and storage still require significant reduction;
- The combustion mechanisms involved in hydrogen co-firing are highly complex, with factors such as injection position, blending ratio, and hydrogen supply method exerting substantial influence on combustion characteristics [142,143];
- The impact of hydrogen on NO_x emission characteristics remains inconclusive;
- Further consideration is also needed for the cost of unit retrofitting.

At present, research efforts are primarily concentrated on the co-firing of hydrogen with gaseous fuels such as natural gas, while investigations and industrial-scale trials involving hydrogen–coal co-firing remain limited.

4.3.1. Large-Scale Deployment of Hydrogen

To achieve the large-scale deployment of hydrogen, progress must be made across its production, transportation, and storage. The commonly used industrial hydrogen production methods, along with their respective advantages and drawbacks, are summarized in Table 3.

Table 3. Industrial hydrogen production.

Production Methods	Advantages	Disadvantages
SMR [144]	Low cost	Generates significant greenhouse gases
Water Electrolysis	Clean production process	High production costs
Coal Gasification [145]	Abundant coal resources and low cost	Generates significant greenhouse gases
Biomass Gasification [146]	Relatively clean production process	Technologically complex and costly

Renewable energy-based water electrolysis for hydrogen production has evolved from the use of curtailed electricity to large-scale deployment. According to the China Hydrogen Energy Development Report (2025), by the end of 2024 more than 600 renewable energy–based water electrolysis hydrogen projects had been planned nationwide, with an installed capacity of approximately 125,000 tonnes per year. Globally, cumulative operational capacity exceeded 250,000 tonnes per year, with China accounting for more than 50% of the total [147]. In recent years, both domestically and internationally, efforts have been actively deploying and constructing large-scale renewable energy-based hydrogen production plants, and some of the commissioned projects are listed in Table 4.

Table 4. Table of Partial Commissioned Renewable Energy-Based Hydrogen Production Projects.

Country	Project Name	Installed Capacity	Key Technology	Hydrogen Purity	Hydrogen Production Capacity
China	China Huadian Megawatt-Scale Green Hydrogen Demonstration Project [148]	120 MW Wind Power and 80 MW Solar PV	Large-scale alkaline electrolyzers and proton exchange membrane (PEM) electrolysis technology	99.9999%	7800 tonnes per year
	Kuqa, Xinjiang Green Hydrogen Demonstration Project [149]	300 MW Solar PV	ten-thousand-ton level water electrolysis hydrogen production processes and integrated engineering technologies	/	20,000 tonnes per year
	Da'an Wind-Solar Powered Green Hydrogen and Ammonia Synthesis Integrated Demonstration Project [150]	700 MW Wind Power and 100 MW Solar PV	Hybrid alkaline–PEM electrolysis for hydrogen production and hydrogen production powered by direct-current microgrids	99.999%	32,000 tonnes per year
The United States	NASA Ames Research Center Green Hydrogen Project [151]	/	4 MW SOEC	/	2.4 tonnes per day
Germany	HY4CHEM Project [152]	54 MW	PEM	/	8000 tonnes per year
Uzbekistan	Tashkent 20 MW Green Hydrogen Project [153]	20 MW Wind Power	PEM	99.99%	3000 tonnes per year

The transportation and storage of hydrogen are also critical steps for achieving large-scale deployment, with common storage and transportation methods summarized in Table 5.

Table 5. Hydrogen Transportation Methods [154].

Transportation Methods	Advantages	Disadvantages
Compressed Gaseous Hydrogen Transportation	Mature technology and well-developed infrastructure; suitable for small- to medium-scale transportation	Hydrogen has a low volumetric energy density, resulting in reduced transportation efficiency, and requires stringent safety standards and high-strength materials.
Liquefied Hydrogen Transportation	High volumetric energy density, suitable for long-distance and large-scale transportation	The liquefaction process is highly energy-intensive and necessitates cryogenic storage tanks and specialized transport equipment, making the technology complex and costly.
Chemical Carrier-Based Hydrogen Transportation	Enables storage and transportation at ambient temperature, with high safety and low transportation costs	Additional chemical processes are required to release hydrogen, leading to low efficiency and increased technological complexity.
Pipeline Transportation of Hydrogen	Suitable for long-distance and large-scale hydrogen transportation, featuring high efficiency	Hydrogen is prone to leakage, thus requiring the use of specialized materials and advanced engineering techniques.

Pipeline transport is the primary option for large-scale hydrogen delivery. At present, the total length of pure hydrogen transmission pipelines worldwide exceeds 5000 km, the United States has constructed approximately 2500 km of hydrogen pipelines [155], while Europe has established around 1770 km [156]. In contrast, China's hydrogen pipeline network is about 400 km, indicating that it is still in the initial development stage [157].

The large-scale application of hydrogen is a critical step in driving the green and low-carbon transition of high-emission industries. However, the green hydrogen industry still faces common challenges, including an incomplete policy framework, technological bottlenecks that require breakthroughs, insufficient infrastructure, and relatively high costs [158]. Technologies for pure hydrogen transport, hydrogen-blended pipeline transmission, and hydrogen storage have achieved notable progress, yet issues remain, such as limited pipeline network coverage and inadequate safety assessment criteria.

4.3.2. Combustion Characteristics of Hydrogen–Coal Co-Firing

At the current stage, there are relatively few studies on hydrogen-coal co-combustion domestically and internationally, and most of these studies are numerical simulations. The research directions mainly focus on H_2-assisted stable combustion at low loads and carbon reduction for coal-fired units, with research objects concentrated on tubular furnaces and pulverized coal furnaces, and the coal types studied are mostly bituminous coal. Liu et al. [159] employed CFD modeling to simulate the operation of a 1000 MW ultra-supercritical coal-fired boiler at 30% load, examining the effects of varying hydrogen and oxygen co-firing ratios in primary air on combustion performance. The results demonstrated that co-firing 5% hydrogen and 10% oxygen effectively elevated flame temperature and mitigated combustion instability under low-load conditions. Colin et al. [160] conducted experiments in a 150-kWh horizontal industrial combustion kiln. Hydrogen was injected through a hydrogen lance, with a hydrogen blending ratio of 30% (which replaces 30% of the coal's energy). The experimental results indicated that the hydrogen lance renders the flame more intense, concentrated, and stable.

Combustion Mechanism

Hydrogen exhibits a high burning velocity and elevated combustion temperature, with a minimum ignition temperature of approximately 520 °C, which is lower than that of most coals. The significant differences in properties between hydrogen and coal (as a gas-solid two-phase fuel), coupled with the influence of factors such as co-firing ratio, hydrogen injection location, and equivalence ratio, lead to a highly complex combustion mechanism in hydrogen–coal co-firing, thereby increasing the research difficulty. At present, mechanistic studies on hydrogen–coal co-firing remain limited both domestically and internationally, necessitating more in-depth research to enhance the accuracy and predictive capability of hydrogen–coal combustion mechanism models.

Hydrogen Blending Ratio

The hydrogen blending ratio is a critical parameter influencing hydrogen–coal co-combustion, as it directly affects flame temperature, flue gas characteristics, and overall combustion efficiency. Wei [143] performed numerical simulations on a 600 MW tangentially fired boiler to investigate the combustion characteristics of coal–sludge–hydrogen co-firing, with hydrogen blending ratios ranging from 20% to 60%. In this configuration, hydrogen replaced part of the secondary air and was introduced through secondary air ducts. The simulation results revealed that the temperature in the main combustion zone decreased gradually with higher hydrogen blending. When the blending ratio increased from 20% to 60% and hydrogen was injected through a single-layer nozzle, the heat flux density in the main combustion zone was reduced by 17.7%. Zhao et al. [161] conducted hydrogen co-firing experiments in a 50 kW down-fired test furnace, increasing the hydrogen blending ratio from 0% to 55%. The results showed that CO_2 emissions decreased continuously with higher hydrogen blending, while both the main combustion zone temperature and the flue gas outlet temperature increased. At a blending ratio of 55%, the main combustion zone temperature was 7.6% higher compared to pure coal combustion.

Regarding the variation trend of the main combustion zone temperature with hydrogen blending ratio, the aforementioned studies have reached contradictory conclusions. The primary reason lies in the differences in research conditions: Zhao et al. [161] conducted experiments under conditions with sufficient oxygen supply, whereas Wei [143] assumed in the numerical simulations that hydrogen partially replaced air, thereby reducing the available oxygen concentration. These findings indicate that oxygen concentration is one of the key parameters influencing combustion behaviour, underscoring the urgent need for further systematic investigations.

Emission Characteristics

In studies on hydrogen–coal co-combustion, researchers have primarily focused on the emission characteristics of pollutants such as NO_x and CO_2, as well as the evolution of flue gas species along the combustion pathway. With the introduction of hydrogen, the carbon content in the fuel decreases, leading to a progressive reduction in CO_2 emissions; the nitrogen content in the fuel also decreases, thereby reducing fuel-NO_x formation. However, the addition of H_2 can alter the formation of prompt-NO_x and thermal-NO_x. Therefore, in hydrogen–coal co-combustion, the impact of hydrogen addition on NO_x emission characteristics has not yet reached a consistent conclusion.

Yang et al. [162] conducted a series of coal–hydrogen co-firing experiments in a 50 kW down-fired combustion test furnace. The results showed that after hydrogen addition, the application of air-staging technology achieved more effective NO emission control compared with pure coal combustion. At a hydrogen blending ratio of 35%, when the overfire air rates were 17%, 39%, and 50%, the outlet NO concentrations were 669.1, 246.8,

and 147.4 mg/m^3, respectively. Johansson et al. [163] investigated the co-combustion characteristics of H_2 and pulverized coal in a 150-kW horizontal industrial furnace. When 30% of the coal (by energy share) was replaced with H_2, the results showed that co-firing reduced CO_2 emissions by 31% compared with pure coal combustion. NO_x emissions averaged 593 mg NO_2/MJ, which was 32% lower than coal-only combustion (915 mg NO_2/MJ) and 78% lower than pure hydrogen combustion (2871 mg NO_2/MJ). Moreover, the injection velocity of hydrogen was found to influence NO_x emissions, with lower velocities resulting in reduced NO_x formation.

Based on the reaction pathways of NO formation from nitrogen-containing fuels and the combustion mechanism of the H_2–O_2 system, the formation and transformation routes of NO_x during hydrogen–coal co-combustion are illustrated in Figure 20 [162,164–166]. Overall, hydrogen co-firing with coal generally reduces the formation of fuel-NO_x and prompt-NO_x, while enhancing the reduction and conversion of NO, thereby lowering the overall NO_x emission level. However, if a high hydrogen blending ratio leads to an elevated flame temperature, thermal-NO_x formation may increase.

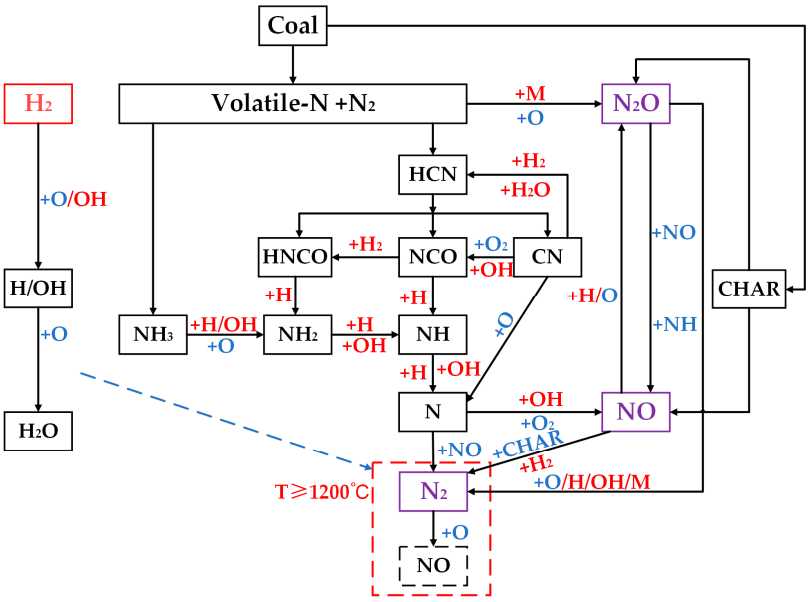


Figure 20. NO_x Formation and Conversion Pathways in the Hydrogen-Coal Co-Combustion Process [162,164–166].

HHO Gas-Coal Co-Combustion

Water electrolysis gas (HHO) refers to a gaseous mixture of hydrogen and oxygen in a volumetric ratio of approximately 2:1, produced via water electrolysis. It was first applied in welding by the Australian engineer Brown. The use of HHO gas generators enables on-demand production and utilization, thereby avoiding the safety risks associated with hydrogen storage [167].

At present, research on the co-combustion of HHO gas and coal remains limited. Zhang et al. [168], using a 0.2 MW down-fired one-dimensional combustion system, investigated the co-combustion of HHO gas with lean coal and lignite. The study examined the influence of HHO injection mode (premixed or staged combustion) and flow rate on combustion intensity and flue gas emissions. The experimental results indicated that: the main combustion zone temperature increased significantly in both cases of HHO–coal co-combustion. With increasing HHO flow, the maximum temperature rise in lean coal–HHO premixed combustion was 108 °C (from 1354 °C to 1462 °C), while in lignite–HHO staged combustion the maximum rise was 95 °C (from 1194 °C to 1289 °C). The variation in NO_x

emissions during co-combustion was governed by the competition between the "NO_x reduction effect of HHO" and the "temperature-induced enhancement of NO_x formation." For lean coal–HHO co-combustion under both modes, NO_x emissions at all flow rates were lower than those of pure coal combustion. With increasing HHO flow, NO_x emissions in lignite–HHO premixed combustion first increased and then decreased, reaching a maximum at an HHO flow of 1100 L/h. Conversely, in lignite–HHO staged combustion, NO_x emissions first decreased and then increased, with a minimum observed at an HHO flow of 2200 L/h. This study provides valuable insights into the application of HHO in utility boilers and its potential role in pollutant control under low-load conditions. Meanwhile, the research team also conducted experiments on the combustion characteristics of HHO gas with staged injection and premixed injection. The experimental results showed that both injection methods could significantly increase the temperature of the main combustion zone; among them, the staged injection method exhibited the optimal NO_x emission reduction effect, which was 97.4% lower than that of pure coal combustion [169].

At present, international research on hydrogen co-firing is primarily focused on blending with natural gas, hydrogen enrichment in gas turbines, or pure hydrogen combustion, while China has further extended these efforts to include hydrogen co-firing with coal. At the Hillabee natural gas power plant, Sterne Energy in the United States achieved a record-setting hydrogen–natural gas co-firing ratio of 38.8%, enabling an annual reduction of approximately 270,000 tonnes of CO_2 emissions [170]. Engineers at Tangshan Sanyou Group Thermal Power Company (Tangshan, China) in China successfully overcame several key challenges, including the development of "process control technologies for hydrogen co-firing in pulverized coal boilers." They achieved stable hydrogen co-firing in Boiler No. 5, which has since been put into operation, resulting in a 0.51% reduction in coal consumption and generating an additional annual economic benefit of over 1.3 million CNY [171].

4.4. Economic Analysis of Coal-Mixed Combustion with Zero-Carbon Fuels

When analyzing the economics of co-firing pulverized coal with zero-carbon fuels, a coal-only operating unit is typically adopted as the baseline scenario, with comprehensive consideration given to fuel supply chain costs, retrofit investment requirements, the impacts of co-firing on unit efficiency, output and operation and maintenance, as well as emission reduction benefits. Commonly used quantitative indicators include the levelized cost of electricity (LCOE), cost per unit of emission reduction, and NPV. By taking co-firing ratios, carbon price levels, and policy incentive intensities as boundary conditions, the applicable scenarios of different zero-carbon fuels in the low-carbon transition of coal-fired power can be clearly identified. Sánchez-Lozano et al. [172] conducted a techno-economic feasibility assessment of a hybrid photovoltaic-assisted biomass gasification combined cooling, heating and power plant deployed in a rural area of the Savannah region of Ghana, showing that the system could achieve a cumulative profit margin of 74%, a payback period slightly below 6.8 years, and an LCOE of USD 0.287 kWh^{-1}. At present, the co-firing of pulverized coal with ammonia or hydrogen remains at the laboratory and pilot-scale research stages, with a lack of large-scale demonstration projects and standardized economic evaluation criteria. Co-firing technologies involving ammonia or hydrogen are still constrained by fuel production and supply costs, upper limits on co-firing ratios, and pressures related to unit efficiency and environmental performance, and therefore require further exploration and technological innovation.

Overall, the strong policy support for large-scale hydrogen deployment and hydrogen co-firing across various countries has significantly accelerated technological advancements in the field. However, numerous technical challenges remain to be addressed, including low-

cost hydrogen production, storage, and transportation; the combustion mechanisms and pollutant control of hydrogen–coal co-firing; issues of corrosion and retrofit requirements associated with high hydrogen blending ratios; and the limited gas production capacity of HHO generators.

5. Conclusions and Outlook

The coupling of large-scale coal-fired power units with renewable energy represents an important measure for advancing the development of a new-type power system and a key pathway for the green and low-carbon transition of coal-fired power. The advantages, challenges, and future development directions of the various technologies are summarized in Table 6.

Overall, coal–renewable coupling technologies remain at the research and development stage, while countries are actively promoting the grid integration of high shares of renewable electricity and the transition of coal-fired power from baseload generation to flexible and ancillary service provision. China is enhancing the coordinated and optimized operation of power sources, vigorously advancing flexibility retrofitting and deep load regulation of coal-fired units, and realizing the value of flexibility through electricity and ancillary services markets [173]. The U.S. Department of Energy has announced plans to allocate USD 100 million to refurbish and upgrade coal-fired power plants [174]. It is believed that, through concerted efforts worldwide, the low-carbon transition of the energy mix and sustainable development will ultimately be achieved.

This review primarily focuses on the generation-side technologies for coupling coal-fired power with renewable energy and does not explicitly address electricity storage and distribution. Future research will place greater emphasis on system-level energy storage and optimal allocation strategies, assess the techno-economic potential of different options, and enhance overall economic feasibility.

Table 6. Summary of Coal-Electricity Coupled Renewable Energy Technology.

Project	Pathway	Technology		Advantages	Challenges	Development Directions
Deep flexible load regulation	Flexibility retrofitting of power units	Stable combustion at low load	Optimization of auxiliary equipment	Minimum stable combustion load of 30–40%	Balancing pulverizer energy consumption and combustion efficiency	Autonomous start-up and shut-down control of pulverizers
			Combustion-supporting measures	Enabling rapid ignition and reducing pollutant emissions	Plasma electrodes exhibit limited adaptability to multi-coal-fuel environments and have a relatively short	Upgrading of electrode materials; intelligent control; optimization of electrode structures
			Novel Combustion Technology	Significantly improving low-load combustion stability and load response rate	Stable operation at ultra-low load	Optimization of burner configuration and retrofit for compatibility with the boiler
			Oxygen-Enriched Combustion	Enhancing combustion intensity and reducing the risk of flame extinction	Heat transfer anomalies, high-temperature corrosion, and high capital investment costs	Breakthroughs in low-cost oxygen production technologies and the development of composite protective coatings for equipment
		Steam turbine system retrofitting		Enhancing unit operational stability, improving load response capability, and protecting critical components	Flow-field distribution of last-stage steam turbine blades under low and variable load conditions, and unit control strategies	Integrated intelligent detection, control, and fault diagnosis technologies
		Fast Startup and Shutdown		Substantially enhancing unit flexibility and increasing load response rate	Reaction kinetics characteristics under non-steady-state conditions, boiler heat-transfer surface safety, and rapid load response technologies, among others	Introducing machine learning, coupling with advanced combustion technologies, and conducting research on multi-coal adaptability

Table 6. *Cont.*

Project	Pathway	Technology	Advantages	Challenges	Development Directions
Deep flexible load regulation	Energy Storage	Physical Energy Storage	Simple operating principle, large capacity, and long service life	Geographical constraints and high upfront investment costs	Improving energy storage efficiency and system integration
		Electrochemical Energy Storage	Fast response speed and high energy density	Relatively high costs and difficulty in achieving large-scale deployment	Developing solid-state batteries and undertaking materials optimization
		Thermal Energy Storage	Long-duration energy storage, large capacity, and abundant resource availability	Low energy efficiency, challenges in high-temperature material compatibility, and difficulties in heat transfer enhancement	Developing system integration technologies and coupling with banked-fire hot standby operation
Co-firing-based emission reduction	Biomass	Direct/Indirect Co-firing	Effectively reducing carbon emissions and promoting resource utilization	Low power generation efficiency, high generation costs, and increased risks of high-temperature corrosion and slagging of equipment	Biomass gasification technologies, optimization of co-firing modes and blending ratios, and synergistic integration with energy storage
	Ammonia	Direct Co-firing	Mature storage and transportation systems, suitable for large-scale energy systems	Difficulties in maintaining stable combustion, highly pronounced NO_x emission issues, and equipment corrosion	Burner retrofitting, coordinated NO_x control technologies, and optimization of high co-firing ratios
	Hydrogen	Direct Co-firing	Significant deep emission reduction potential, improved pulverized coal ignition and stable combustion, and facilitation of rapid start-up and shut-down	Incomplete storage, transportation, and supply infrastructures, high combustion safety risks, and significant challenges in NO_x control	Optimization of burner and furnace configurations, multi-fuel synergy technologies, and coupling with energy storage

Author Contributions: Writing—original draft, Y.H.; Writing—review & editing, Z.O. and H.D.; Supervision, Z.O. and H.D.; Project administration, H.D.; Formal analysis, Y.H.; Validation, Y.H. and H.D.; Investigation, Y.H., H.W., S.L. and L.W.; Data curation, Y.H. All authors have read and agreed to the published version of the manuscript.

Funding: This research was funded by the Youth Training Program of the State Key Laboratory of Coal Conversion [2025BWZ002], Strategic Priority Research Program of CAS [XDA29010200], and the Youth Innovation Promotion Association of CAS [Y2023044].

Data Availability Statement: The original contributions presented in the study are included in the article; further inquiries can be directed to the corresponding authors.

Conflicts of Interest: The authors declare no conflicts of interest.

Abbreviations

The following abbreviations are used in this manuscript:

APS	Automatic Procedure Startup/Shutdown System
BESS	Battery Energy Storage System
BP	Booster Pump
CFPP	Coal-Fired Power Plant
CFB	Circulating Fluidized Bed
CFD	Computational Fluid Dynamics
CWP	Cooling Water Pump
CAS	Chinese Academy of Sciences
CNY	Chinese Yuan
CAES	Compressed Air Energy Storage
C	Compressor
CON	Condenser
CS	Cold Storage
CCS	Carbon Capture and Storage
DEA	Deaerator
EUR	Euro
E	Expander
FWP	Feed Water Pump
FESS	Flywheel Energy Storage Systems
G	Generator
HV	The Standard Symbol for Vickers Hardness
HPT	High-Pressure Turbine
HST	High-Pressure Storage Tank
HHO	Hydrogen-Oxygen Mixture (Hydroxy Gas)
IPT	Intermediate-Pressure Turbine
IC	Intercooler
IP	Intermediate Pressure
IRR	Internal Rate of Return
IPP	Investment Payback Period
JERA	Kabushikigaisha JERA
LQC	Low-Quality Coal
LPT	Low-Pressure Turbine
LST	Low-Pressure Storage Tank
LP	Low-Pressure
LIBES	Lithium-Ion Battery Energy Storage
LCOE	Levelized Cost of Electricity
M	Motor
MSTES	Molten Salt Thermal Energy Storage
NO_x	Nitrogen Oxides

NPV	Net Present Value
PH	Preheater
PV	Photovoltaic
PEM	Proton Exchange Membrane
R&D	Research and Development
RFBES	Redox Flow Battery Energy Storage
SCR	Selective Catalytic Reduction
SFS	Supersonic Flame Spraying
SPTES	Solid Particle Thermal Energy Storage
SMR	Steam Methane Reforming
SOEC	Solid Oxide Electrolysis Cell
SO_x	Sulfur Oxides
TV	Throttle Valve
THA	Turbine Heat Acceptance
TCES	Thermochemical energy storage
USD	United States Dollar

References

1. IEA. Electricity 2025 (Analysis and Forecast to 2027). Available online: https://www.iea.org/reports/electricity-2025 (accessed on 16 December 2025).
2. Pyshyev, S.; Prysiazhnyi, Y.; Shved, M.; Namiesnik, J.; Bratychak, M. State of the art in the field of emission reduction of sulphur dioxide produced during coal combustion. *Crit. Rev. Environ. Sci. Technol.* **2017**, *47*, 2387–2414. [CrossRef]
3. China Petrochemical News. Report on the Transformation of the U.S. Energy Structure: Retirement of Coal Power and Rise of Solar and Battery Storage. Available online: http://www.sinopecnews.com.cn/xnews/content/2025-03/28/content_7122243.html (accessed on 24 September 2025).
4. Ministry of Commerce of the People's Republic of China. Report on the Proportion of Renewable Electricity Generation in the EU Reaching 47% in 2024. Available online: https://chinawto.mofcom.gov.cn/article/ap/p/202504/20250403574754.shtml (accessed on 24 September 2025).
5. China Energy Media Research Institute. China Energy Big Data Report (2025)-Comprehensive Energy Chapter. Available online: https://gdshe.org/article/25052.html (accessed on 16 December 2025).
6. Shi, M.; Liu, J.; Guo, H.; Jiang, N.; Lai, X.; Kang, C. Analysis of Causes and Countermeasures for Negative Electricity Prices in Power Systems with a High Penetration of New Energy. *Autom. Electr. Power Syst.* **2025**, 1–16.
7. Wang, X.; Li, Y.; Li, J. Deep Peak Regulation of Thermal Power under Renewable Integration. In Proceedings of the 2025 Annual Proceedings of Beijing Society of Electrical Engineering, 2025 Annual Conference of China Society for Electrical Engineering, Changsha, China, 24–27 November 2025. [CrossRef]
8. Yang, D.; Lv, Y.; Ji, M. Evaluation and economic analysis of battery energy storage in smart grids with wind-photovoltaic. *Int. J. Low-Carbon Technol.* **2024**, *19*, 18–23. [CrossRef]
9. Solarte-Toro, J.C.; González-Aguirre, J.A.; Giraldo, J.; Alzate, C. Thermochemical processing of woody biomass: A review focused on energy-driven applications and catalytic upgrading. *Renew. Sustain. Energy Rev.* **2021**, *136*, 110376. [CrossRef]
10. National Development and Reform Commission of the People's Republic of China. Action Plan for the Low-Carbon Transformation and Construction of Coal-Fired Power Generation (2025–2027). Available online: https://www.nea.gov.cn/20250418/5c9e2108eefc4e7d8c9931de4456dda9/c.html (accessed on 22 December 2025).
11. Brinkman, G.; Bain, D.; Buster, G.; Draxl, G.; Das, P.; Ho, J. The North American Renewable Integration Study: A U.S. Perspective. Available online: https://docs.nrel.gov/docs/fy21osti/79224.pdf (accessed on 16 December 2025).
12. Peng, D.; Wang, B.; Cai, X.; Bei, L. Research on the Modification of Coal Adaptability and Carbon Emissions Reduction Technology for Coal-Fired Boilers. *Energies* **2022**, *15*, 9533. [CrossRef]
13. Ouyang, Z.; Wang, H.; Lyu, Q.; Zhu, S.; Zeng, X.; Su, K. Research Progress on Deep Peak Shaving Technology of Pulverized Coal-fired Boiler Power Unit. *Proc. CSEE* **2023**, *43*, 8772–8790. [CrossRef]
14. Chen, H.; Wang, A.; Dai, W.; Cai, P.; Ran, C. Study on Effect of Pulverized Coal Fineness on Combustion Characteristics and Low Load Stable Combustion of High Ash Bituminous Coal. *Power Syst. Eng.* **2020**, *36*, 13–15.
15. Liu, W.; Wang, S.; Wu, J.; Song, D.; Gao, W. Experimental Study on Low Load Operation Optimization of 350 MW Supercritical Unit. *Northeast Electr. Power Technol.* **2021**, *42*, 5–8+52.
16. Ang, Y. Adjustment Technology Analysis of Deep Cyclic Operation Optimization of 350 MW Supercritical Unit. *Inn. Mong. Electr. Power* **2018**, *36*, 32–36.

17. Song, M.; Huang, M.; Huang, Q.; Li, S. Discussion on Low-load Stable Combustion Technology of Swirl Pulverized-coal Burner. *Proc. CSEE* **2021**, *41*, 4552–4566. [CrossRef]
18. Huang, C.; Li, Z.; Lu, Y.; Wang, Y.; Chen, Z. Gas-solid flow characteristics of a new low-load stable combustion burner. *Clean Coal Technol.* **2025**, *31*, 218–228. [CrossRef]
19. Wang, Y.; Li, Z.; Huang, C.; Liu, H.; Feng, Y.; Du, X. Influence of central coal feed swirl combustion technology on wide-load range performance of burners, based on gas/particle flow characteristics. *Energy* **2025**, *320*, 135404. [CrossRef]
20. Qiang, S.; Yv, J. Economic Analysis of the Application of Micro-Oil Ignition Technology in Small-Scale Pulverized Coal-Fired Boilers. *Sci. Technol. Innov.* **2020**, *10*, 162–163.
21. Wei, C.; Guo, Z. Research on Operation and Commissioning of Boiler Micro-Oil Ignition Technology. *Boil. Manuf.* **2024**, *5*, 3–5.
22. Yang, M.; Han, Z.; Wang, W.; Liu, X.; Liu, J. Application Practice of Micro-Oil Ignition Technology in 100% Anthracite Coal Production Lines. *Cement* **2023**, *10*, 33–35. [CrossRef]
23. Zhang, L.; Yv, J.; Zhao, B.; Zhang, D.; Wang, X.; Hu, Y. Study on Ignition and Combustion Characteristics of Gliding Arc Plasma Combustion Dome. *J. Eng. Thermophys.* **2025**, *46*, 300–309.
24. Askarova, A.; Safarik, P.; Bolegenova, S.; Nugymanova, A.; Maximov, V.; Askarov, N. Using Plasma Activation to Optimize the Combustion Process and Minimize Harmful Emissions. *Chem. Eng. Technol.* **2021**, *44*, 1970–1977. [CrossRef]
25. Li, M.; Zou, P.; Li, B.; Cai, W.; Cheng, Z.; Liu, X. Application of plasma ignition technology in 660 MW high moisture lignite unit. *Clean Coal Technol.* **2024**, *30*, 52–59. [CrossRef]
26. Shen, T.; Song, M.; Huang, Y.; Zhu, R.; Li, Z.; Yu, Q. The effectiveness of a novel coal-igniting-fuel technology and application in a direct current burner. *Fuel* **2021**, *306*, 121503. [CrossRef]
27. Lyu, Q.; Zhu, J.; Ouyang, Z.; Zhu, S. *Principles and Technologies of Preheated Combustion*, 1st ed.; Science Press: Beijing, China, 2023; pp. 9–18.
28. Wang, H.; Ding, H.; Ouyang, Z.; Li, S.; Su, K.; Chen, Q. Experimental study on peak shaving operations for efficient pulverized coal combustion and working fluid coordination. *Fuel* **2026**, *404*, 136237. [CrossRef]
29. Hui, J.; Zhu, S.; Li, Z.; Lin, J.; Cao, X.; Lyu, Q. Experimental study on peak shaving during preheating combustion for different coal ranks: Thermal modification and variable load operation. *Fuel* **2024**, *373*, 132324. [CrossRef]
30. Ding, H.; Li, S.; Ouyang, Z.; Zhu, S.; Zeng, X.; Wang, H. Study on Combustion and NO_x Emission Characteristics of Low-Quality Coal with Wide Load Based on Fuel Modification. *Energies* **2025**, *18*, 2798. [CrossRef]
31. Zhu, J.; Han, H.; Li, D.; Liu, J.; Lyu, Q. The Demonstration of 240 t/h Circulating Fluidized Bed Boiler with Deeply Flexible Peak-shaving. *China Spec. Equip. Saf.* **2024**, *40*, 89–93.
32. Shanxi Institute of Coal Chemistry; Chinese Academy of Sciences. Coal Gasification Coupling with Stable Combustion Technology for Pulverized Coal-Fired Boilers Facilitates 20% Low-Load Deep Peak Shaving of Pulverized Coal-Fired Boilers. Available online: https://sxicc.cas.cn/news/kjcx/202405/t20240511_7158053.html (accessed on 25 September 2025).
33. Zhang, H.; Lin, H.; Zhou, X.; Wang, X.; Zheng, H.; Liu, Y. CFD modeling and industry application of a self-preheating pulverized coal burner of high coal concentration and enhanced combustion stability under ultra-low load. *Appl. Therm. Eng.* **2024**, *253*, 123831. [CrossRef]
34. Yao, G.; Han, X.; Liu, Z.; Tang, H.; Zhou, Y.; Wang, Z. Low-NO_x study of a 600 MW tangentially fired boiler based on pulverized coal preheating method. *Case Stud. Therm. Eng.* **2023**, *48*, 103156. [CrossRef]
35. Yang, Y.; Zhang, Y.; Cai, L.; Wei, M.; Li, D. Analysis on Industrial Application Progress of Oxygen Enriched Combustion. *Energy Energy Conserv.* **2021**, *7*, 179–181+205.
36. Skryja, P.; Hudak, I.; Bojanovsky, J.; Jegla, Z.; Korcek, L. Effects of Oxygen-Enhanced Combustion Methods on Combustion Characteristics of Non-Premixed Swirling Flames. *Energies* **2022**, *15*, 2292. [CrossRef]
37. Tian, H.; Guo, Y.; Wang, P.; Niu, L.; Chen, A.; Zhang, X. Experimental Study on the Effect of Oxy-Fuel Combustion on the Stable Combustion Performance of Boilers under the Background of Deep Peak Shaving. *Energy Conserv.* **2024**, *43*, 118–121.
38. Lun, X.; Xin, H.; Li, H.; Liu, P.; Ding, J.; Zhang, Y. Numerical Simulation of Oxygen-enriched Co-combustion Characteristics of Recycled Submerged Arc Furnace Gas and Pulverized Coal in Rotary Kiln. *J. Mater. Metall.* **2025**, 1–16. Available online: https://link.cnki.net/urlid/21.1473.tf.20250911.0927.002 (accessed on 25 September 2025).
39. Wang, Y.; Zhou, Y. Equipment capacity matching methodology and techno-economic analysis for a novel low-carbon multi-energy system with the integration of oxy-coal combustion power plant and power-to-gas. *Energy* **2025**, *322*, 135693. [CrossRef]
40. Shi, Y.; Zhong, W.; Shao, Y.; Liu, X. Energy efficiency analysis of pressurized oxy-coal combustion system utilizing circulating fluidized bed. *Appl. Therm. Eng.* **2019**, *150*, 1104–1115. [CrossRef]
41. Liu, Q.; Zhang, Y.; Ye, H.; Zhou, G.; Su, Y.; Dong, W. Combustion behavior and pollutant emissions of the pressurized fluidized bed oxy-fuel co-firing of coal and poultry manure. *Chin. J. Chem. Eng.* **2025**, *83*, 171–181. [CrossRef]
42. Symonds, R.T.; Hughes, R.W.; Loscertales, M.D. Oxy-pressurized fluidized bed combustion: Configuration and options analysis. *Appl. Energy* **2020**, *262*, 114531. [CrossRef]

43. Chen, H. First Megawatt-Scale Staged Pressurized Oxygen-Enriched Combustion Pilot Plant Has Set Multiple Records. *China Sci. Dly.* **2025**, *003*.
44. Xing, Z. Transformation and Optimization of Steam Turbine Control System of Ultra-Supercritical Unit. *Electr. Power Equip. Manag.* **2025**, *9*, 110–112.
45. Zhu, G.; Guo, D.; Li, J.; Xie, Y.; Zhang, D. Intelligent steam turbine start-up control based on deep reinforcement learning. *Energy* **2025**, *320*, 135335. [CrossRef]
46. Han, X.; Li, Q.; Li, M.; Yao, B.; Han, Z. Flow characteristics and backpressure optimization of low-pressure stages in steam turbines under low flow rate conditions. *Appl. Therm. Eng.* **2025**, *278*, 127415. [CrossRef]
47. Liang, D.; Li, N.; Zhou, Z.; Li, Y. Effect of the water erosion on the non-equilibrium condensation in steam turbine cascade. *Int. J. Heat Mass Transf.* **2025**, *236*, 126326. [CrossRef]
48. Hu, P.; Meng, Q.; Fan, W.; Gu, W.; Wan, J.; Li, Q. Vibration characteristics and life prediction of last stage blade in steam turbine Based on wet steam model. *Eng. Fail. Anal.* **2024**, *159*, 108127. [CrossRef]
49. Liu, Y.; Xie, Y.; Sun, Q.; Fan, Z. Study on Flutter Characteristics of Last-Stage Blades in Steam Turbines Under Deep Peak Shaving Conditions. *Therm. Turbine* **2025**, *54*, 79–84.
50. Mei, L.; An, C.; Ye, X. Application of High Velocity Oxygen Fuel Coating Against Droplet Erosion for Turbine Blade. *Therm. Turbine* **2022**, *51*, 214–218.
51. Abdullah, M.A.; Hadi, R.Z.; Darweesh, S.Y. Protection of turbine blades by adding metals to ceramic materials using flame coating method. *J. King Saud Univ.-Eng. Sci.* **2024**. [CrossRef]
52. Dong, F.; Cheng, L.; Li, Z.; Bai, X. Numerical Simulation and Experimental Study on Optimal Adjustment of Stable Combustion of Subcritical Forced Circulation Boiler at 20% Low Load. *J. Eng. Therm. Power* **2022**, *37*, 117–127.
53. China Energy Engineering Group Tianjin Electric Power Construction Co., Ltd. Brief Report on the Flexible Regenerative Heating Renovation Project of Jiangsu Jianbi Power Plant, National Energy Group. Available online: http://mm.chinapower.com.cn/dww/yxjx/20240606/249117.html (accessed on 25 September 2025).
54. Wang, Z.; Li, L.; You, Y.; Yan, R.; Gu, Y. High and low pressure cylinder bypass heat supply unit operation characteristics with coordinated intermediate pressure valve control. *Case Stud. Therm. Eng.* **2025**, *75*, 107131. [CrossRef]
55. Chen, K. Research on the Windage Condition and Cooling Safety of the Flow Passage of the Low-Pressure Cylinder of Zero-Output Operation Steam Turbine. Master's Thesis, Shandong University, Jinan, China, May 2023.
56. Lu, S.; Wang, Z.; Zhao, Z.; Xu, H.; Gu, Y. Characteristic Analysis of the Unit with Low-pressure Cylinder Zero-output Integrated with Heat Storage Tank. *J. Chin. Soc. Power Eng.* **2025**, *45*, 953–960.
57. He, G. Optimization of Auto-start-stop Control for Deep Peak-shaving Operation of Thermal Power Plant. *Electr. Eng.* **2023**, *9*, 203–206+209.
58. Qiao, L.; Wang, X.; Nie, H.; Liu, C.; Wei, S.; Hao, H. Investigation on the Operation Characteristics of Circulating Fluidized Bed Boiler Unit for Full-load Regulation. *Proc. CSEE* **2025**, *45*, 184–194.
59. Guo, X.; Yu, J. Research and Application of Emergency Start-stop Peak Regulation of Large CFB Boilers. *Appl. Energy Technol.* **2023**, *11*, 28–32.
60. Lyu, J.; Jiang, L.; Ke, X.; Zhang, H.; Liu, Q.; Huang, Z. Future of circulating fluidized bed combustion technology in China for carbon neutralization. *Coal Sci. Technol.* **2023**, *51*, 514–522.
61. Wang, H.; Song, G.; Song, W. Research of CFB boiler banked fire for heat standby and rapid startup peak regulation technology. *J. China Coal Soc.* **2025**, *50*, 4502–4515.
62. Cheng, F.; Zhang, P.; Zhang, Y.; Zhao, M.; Xv, S.; Jia, Y. A Method of Intermittent Banked Fire Near-Zero Ultra-Long Depth Peaking for a Sub-critical CFB Unit. CN117450495A, 26 January 2024.
63. Song, H.; Wang, J.; An, Z.; Lan, W.; Cheng, J.; Guo, J. Experimental study on start-stop peak regulation of a 350 MW supercritical circulating fluidized bed coal-fired power unit. *Therm. Power Gener.* **2025**, *54*, 63–70.
64. Dong, B.; Li, Y.; Ma, L.; Xu, Y.; Zhao, B.; Yang, J. Experimental study on banked fire for peak regulation of supercritical circulating fluidized bed units. *Therm. Power Gener.* **2025**, *54*, 82–90.
65. Fu, J.; Zhu, S.; Liu, Y.; Sun, Y.; Chai, Z.; Gao, M. Case analysis of combustion-side flexibility retrofit schemes based on a framework for technical economy of coal-fired unit. *Energy* **2025**, *339*, 139077. [CrossRef]
66. Meng, Y.; Cao, Y.; Li, J.; Liu, C.; Li, J.; Wang, Q. The real cost of deep peak shaving for renewable energy accommodation in coal-fired power plants: Calculation framework and case study in China. *J. Clean. Prod.* **2022**, *367*, 132913. [CrossRef]
67. Xu, J.; Zhang, Q.; Ye, N.; Zhang, Z.; Wu, X.; Fan, H. A review on flexible peak shaving development of coal-fired boilers in China under the carbon peak and carbon neutrality goals. *Therm. Sci. Eng. Prog.* **2024**, *55*, 103004. [CrossRef]
68. Geweda, A.; Saif, A.; Zayed, M.; Kabeel, A.; Zafar, S.; Khalid, M. Recent advances in hybrid compressed air energy storage systems: Technology categorization, integration potentials with renewable energy systems, and retrofitting improvement strategies. *Alex. Eng. J.* **2025**, *115*, 12–29. [CrossRef]

69. Zhang, Y.; Zuo, Z.; Zhou, X.; Guo, W.; Chen, H. Comparative Analysis of Diagonal and Centrifugal Compressors with Synergy Theory in Compressed Air Energy Storage System. *J. Therm. Sci.* **2024**, *33*, 1325–1339. [CrossRef]
70. Shi, X.; He, Q.; Liu, Y.; An, X.; Zhang, Q.; Du, D. Thermodynamic and techno-economic analysis of a novel compressed air energy storage system coupled with coal-fired power unit. *Energy* **2024**, *292*, 130591. [CrossRef]
71. Shi, X.; He, Q.; Liu, Y.; Zhang, Q.; An, X.; Du, D. Design and analysis of a novel liquefied air energy storage system coupled with coal-fired power unit. *J. Energy Storage* **2023**, *73*, 109204. [CrossRef]
72. Wang, Y.; Lyu, K.; Ma, T.; Ju, W.; Zhang, J.; Xu, P. Analysis of compressed air energy storage system coupled with coal-fired power unit. *Therm. Power Gener.* **2021**, *50*, 54–63.
73. Hou, K.; Wang, Y.; Han, N.; Ma, T.; Lv, K.; Liu, X. Performance analysis of a liquid carbon dioxide energy storage system integrated with a coal-fired power plant. *J. Energy Storage* **2024**, *77*, 109869. [CrossRef]
74. Song, S.; Qiao, T.; Zhang, R.; Liang, S.; Liu, Y. Simulation study of flywheel energy storage assisted coal-fired unit frequency regulation. *Bull. Pol. Acad. Sci.-Tech. Sci.* **2024**, *72*, e151951. [CrossRef]
75. Elbouchikhi, E.; Amirat, Y.; Feld, G.; Benbouzid, M.; Zhou, Z. A Lab-scale Flywheel Energy Storage System: Control Strategy and Domestic Applications. *Energies* **2020**, *13*, 653. [CrossRef]
76. Tasneem, O.; Tasneem, H.; Xian, X. Lithium-ion Battery Technologies for Grid-scale Renewable Energy Storage. *Next Res.* **2025**, *2*, 100297. [CrossRef]
77. Cao, X.; Yan, X.; Zhao, K.; Ke, L.; Jiang, X.; Li, L. Simple electrode assembly engineering: Toward a multifunctional lead-acid battery. *J. Energy Chem.* **2024**, *96*, 536–543. [CrossRef]
78. Zheng, N.; Wang, Q.; Ding, X.; Zhang, H.; Duan, L.; Wang, X. Techno-economic analysis of a novel solar-based polygeneration system integrated with vanadium redox flow battery and thermal energy storage considering robust source-load response. *Appl. Energy* **2024**, *376*, 124288. [CrossRef]
79. Yang, S.; Shao, C.; Xiao, X.; Fang, D.; Li, N.; Zhao, E. Revealing stable organic cathode/solid electrolyte interface to promote all-solid-state sodium batteries using organic cathodes. *Energy Storage Mater.* **2024**, *73*, 103857. [CrossRef]
80. Zhang, S.; Li, Y.; Du, E.; Fan, C.; Wu, Z.; Yao, Y. A review and outlook on cloud energy storage: An aggregated and shared utilizing method of energy storage system. *Renew. Sustain. Energy Rev.* **2023**, *185*, 113606. [CrossRef]
81. Xiu, X.; Li, J.; Hui, D. Sizing and Economic Analysis of Lithium-ion Battery Energy Storage System. *Adv. Energy Sci. Technol.* **2013**, *291–294*, 627–631. [CrossRef]
82. Chang, X.; Zhao, Y.; Yuan, B.; Fan, M.; Meng, Q.; Guo, Y. Solid-state lithium-ion batteries for grid energy storage: Opportunities and challenges. *Sci. China-Chem* **2024**, *67*, 43–66. [CrossRef]
83. Si, H.; Ma, J.; Xia, X.; Wang, Q.; Geng, S.; Fu, L. Solid-State Sodium-Ion Batteries: Theories, Challenges and Perspectives. *Chem. Eur. J.* **2025**, *31*, e202403247. [CrossRef]
84. Zhao, S.; Li, G.; Zhang, B.; Li, T.; Luo, M.; Sun, B. Technological roadmap for potassium-ion hybrid capacitors. *Joule* **2024**, *8*, 922–943. [CrossRef]
85. Tan, A.K.X.; Paul, S. Beyond Lithium: Future Battery Technologies for Sustainable Energy Storage. *Energies* **2024**, *17*, 5768. [CrossRef]
86. Kuzmin, I.; Loskutov, A.; Osetrov, E.; Kurkin, A. Source for Autonomous Power Supply System Based on Flow Battery. *Energies* **2022**, *15*, 3027. [CrossRef]
87. Liu, Y.; Wang, Y.; Bai, X.; Li, X.; Ning, Y.; Song, Y. Review on modeling and control of megawatt liquid flow energy storage system. *Energy Rep.* **2023**, *9*, 113–123. [CrossRef]
88. Holland-Cunz, M.V.; Cording, F.; Friedl, J.; Stimming, U. Redox flow batteries—Concepts and chemistries for cost-effective energy storage. *Front. Energy* **2018**, *12*, 198–224. [CrossRef]
89. Ouyang, T.; Zhang, M.; Qin, P.; Tan, X. Flow battery energy storage system for microgrid peak shaving based on predictive control algorithm. *Appl. Energy* **2024**, *356*, 122448. [CrossRef]
90. Sharmoukh, W. Redox flow batteries as energy storage systems: Materials, viability, and industrial applications. *RSC Adv.* **2025**, *15*, 10106–10143. [CrossRef] [PubMed]
91. Vallese, L.; Javadi, H.; Badenes, B.; Urchueguia, J.F.; Lombardo, G.; Menegazzo, D. A comprehensive review of thermal energy storage technologies and their applications: Creation of a database. *Renew. Sustain. Energy Rev.* **2026**, *225*, 116133. [CrossRef]
92. Yong, Q.; Tian, Y.; Qian, X.; Li, X. Retrofitting coal-fired power plants for grid energy storage by coupling with thermal energy storage. *Appl. Therm. Eng.* **2022**, *215*, 119048. [CrossRef]
93. Sun, C.; Zhai, R.; Wang, Y.; Xu, Y.; Li, J. Design and Performance Analysis of Flexibility Peaking System for Coal-fired Power Plant Based on Solar-Molten Salt Energy Storage. *J. Therm. Sci.* **2025**, *34*, 1223–1240. [CrossRef]
94. Li, B.; Cao, Y.; He, T.; Si, F. Thermodynamic analysis and operation strategy optimization of coupled molten salt energy storage system for coal-fired power plant. *Appl. Therm. Eng.* **2024**, *236*, 121702. [CrossRef]
95. Liu, M.; Miao, L.; Wang, Z.; Yan, J. Design and thermo-economic analysis on molten salt thermal energy storage system integrated within coal-fired power plant: Co-storing energy from live and reheat steam. *J. Energy Storage* **2025**, *131*, 117637. [CrossRef]

96. Ma, Z.; Wang, X.; Davenport, P.; Gifford, J.; Martinek, J. Economic analysis of an electric thermal energy storage system using solid particles for grid electricity storage. ASME 15th International Conference on Energy Sustainability (ES), Online, 16–18 June 2021.
97. Liu, X.; Li, H.; Lv, L.; Wei, L.; Zhou, H. Experimental study on single-unit solid particle packed bed for thermal energy storage of extracted steam from thermal power plant to consume more renewable energy. *Particuology* **2025**, *97*, 99–116. [CrossRef]
98. Shank, K.; Tiari, S. A Review on Active Heat Transfer Enhancement Techniques within Latent Heat Thermal Energy Storage Systems. *Energies* **2023**, *16*, 4165. [CrossRef]
99. Wang, C.; Wang, S.; Cheng, X.; Zhang, Y.; Wang, Z. Research progress and performance improvement of phase change heat accumulators. *J. Energy Storage* **2022**, *56*, 105884. [CrossRef]
100. World's First 300-Megawatt CAES National Demonstration Power Station Achieves Grid-Connected Power Generation. Available online: https://www.cas.cn/cm/202405/t20240506_5013598.shtml (accessed on 28 September 2025).
101. World's First Set of 660 MW Man-Made Cavern-Type CAES Project Commences Construction. Available online: https://news.cctv.com/2025/05/11/ARTIIUd4S3Q2BQ2FvURwZEmQ250511.shtml (accessed on 28 September 2025).
102. World's Largest Single-Unit Maglev FESS Project at Penglai Company in Shandong Achieves Grid-Connected Commissioning. Available online: https://www.chnenergy.com.cn/gjnyjtww/chnjcxw/202501/69f076534cea4c4aa82c297d33e54c26.shtml (accessed on 28 September 2025).
103. Global First Set of MW Iron-Chromium FBES Demonstration Project Completes Construction in Inner Mongolia. Available online: http://www.spic.com.cn/xtdt1/202302/t20230224_321035.html (accessed on 28 September 2025).
104. 250MW/1000MWh! Grid-Forming AVFBES Project of Wushi Energy Storage Power Station, Aksu, Xinjiang Successfully Passes Artificial Short-Circuit Test in One Go. Available online: https://www.escn.com.cn/news/show-2132399.html (accessed on 28 September 2025).
105. The Electrical Energy Storage Frequency Regulation Project of Shaanxi Coal Power Yuncheng Co., Ltd. Achieves Grid-Connection as Scheduled. Available online: https://m.bjx.com.cn/mnews/20240425/1373556.shtml (accessed on 22 December 2025).
106. China's Largest "Thermal Power + Molten Salt" Energy Storage Project Completes Construction of Its Main Structure. Available online: https://www.chnenergy.com.cn/gjnyjtww/chnjtyw/202503/e9a2bf48931d42339a89e7fc9097a65b.shtml (accessed on 28 September 2025).
107. The Institute of Engineering Thermophysics (CAS) Makes New Progress in MW-Scale High-Temperature Solid Particle Heat Storage Pilot-Scale Research. Available online: https://iet.cas.cn/news/kyjz/202509/t20250924_7976813.html (accessed on 28 September 2025).
108. Bai, T.; Shi, W.; Shi, W.; Zheng, L.; Xu, G.; Zhang, M. Thermodynamic and economic analysis of the compressed air energy storage coupled with the combustible solid waste power plant. *J. Energy Storage* **2026**, *141*, 119345. [CrossRef]
109. Grimaldi, A.; Minuto, F.; Perol, A.; Casagrande, S.; Lanzini, A. Techno-economic optimization of utility-scale battery storage integration with a wind farm for wholesale energy arbitrage considering wind curtailment and battery degradation. *J. Energy Storage* **2025**, *112*, 115500. [CrossRef]
110. Report on the Development of China's Biomass Briquette Fuel Industry in 2025. Available online: http://www.beipa.org.cn/newsinfo/8793616.html (accessed on 29 October 2025).
111. Liu, G.; Zeng, J.; Ran, S.; Li, X.; Zhang, X.; Guo, G. Research and engineering application on the influence of large-scale direct coupled biomass in pulverized coal boiler. *Clean Coal Technol.* **2024**, *30*, 237–242. [CrossRef]
112. Zhao, X.; Tu, A.; Chen, E.; Zhu, D. Research Status and Prospect of the Influence of Direct Coupling Biomass on Coal-fired Power Generation System. *Biomass Chem. Eng.* **2025**, *59*, 57–66.
113. Jiang, Y.; Wang, F.; Xue, W.; Li, Z.; Zhang, Y.; Fan, Y. Study on the Co-combustion Characteristics of Biomass and Coal. *Energy Sci. Technol.* **2022**, *20*, 44–48.
114. Key Technological Breakthrough in 25% High-Proportion Co-Firing of Giant Reed Pellets in Single Mill of 1000MW Unit. Available online: https://www.csee.org.cn/portal/xpqyzx/20250217/34458.html (accessed on 28 September 2025).
115. China's First Test of "Large-Scale Coal-Fired Power Unit Cow Dung Co-Firing" Successfully Completes. Available online: https://wenming.xlgl.gov.cn/wenming/xwzx/jjwm/2024092909275167289/index.html (accessed on 28 September 2025).
116. Zhang, D.; Zhou, T.; Zhang, Y.; Zhu, S.; Li, D.; Yang, H.; Zhang, M. Analysis of Technical Scheme of Coupled Biomass Power Generation in Coal-fired Units. *J. Electr. Power* **2025**, *40*, 171–181.
117. Fan, L.; Chen, H.; Gao, Y.; Zhao, H.; Yao, L.; Li, Y. Performance analysis of a novel power generation design containing the drying and Co-gasification of sludge and biomass integrated with the waste heat recovery of a cement plant. *Energy* **2025**, *326*, 136331. [CrossRef]
118. Chen, X. Performance Analysis and Simulation Optimization of Biomass Gasification Coupled Coal-Fired Power Plant System Based on Waste Heat and Water Recovery. Master's Thesis, Huazhong University of Science and Technology, Wuhan, China, 14 May 2024.
119. Han, W. Combustion Characteristics and Pollutant Emissions of Biomass (Gas) Coupled with a Coal-Fired Boiler. Master's Thesis, North China University of Water Resources and Electric Power, Zhengzhou, China, May 2022.

120. Al-Qayim, K.; Nimmo, W.; Pourkashanian, M. Comparative techno-economic assessment of biomass and coal with CCS technologies in a pulverized combustion power plant in the United Kingdom. *Int. J. Greenh. Gas Control* **2015**, *43*, 82–92. [CrossRef]
121. Xie, S.; Yang, Q.; Wang, Q.; Zhou, H.; Bartocci, P.; Fantozzi, F. Coal power decarbonization via biomass co-firing with carbon capture and storage: Tradeoff between exergy loss and GHG reduction. *Energy Convers. Manag.* **2023**, *288*, 117155. [CrossRef]
122. National Action Plan for Low-Carbon Transformation and Construction of Coal-Fired Power (2024–2027 Annual). Available online: https://www.ndrc.gov.cn/xxgk/zcfb/tz/202407/t20240715_1391663.html (accessed on 28 September 2025).
123. Toward Zero-Emission Thermal Power Plants. Available online: https://www.enecho.meti.go.jp/category/others/for_energy_technology/pdf/pamphlet_0201.pdf (accessed on 28 September 2025).
124. Choo, H.; Kim, Y.; Kim, D. Power sector carbon reduction review for South Korea in 2030. *Renew. Sustain. Energy Rev.* **2024**, *196*, 114348. [CrossRef]
125. Liu, M.; Chen, S.; Zhu, H.; Zhou, Z.; Xu, J. Numerical investigation of ammonia/coal co-combustion in a low NO_x swirl burner. *Energy* **2023**, *282*, 128358. [CrossRef]
126. Lee, B.; Bae, Y.; Cho, S.; Kim, G.; Jeon, H. Comprehensive technical review for fundamental characteristics and application of NH_3 co-firing with coal. *Chem. Eng. J.* **2023**, *474*, 145587. [CrossRef]
127. Hadi, K.; Ichimura, R.; Hashimoto, G.; Xia, Y.; Hashimoto, N.; Fujita, O. Effect of fuel ratio of coal on the turbulent flame speed of ammonia/coal particle cloud co-combustion at atmospheric pressure. *Proc. Combust. Inst.* **2021**, *38*, 4131–4139. [CrossRef]
128. Zhang, M.; Wei, X.; An, Z.; Okafor, E.C.; Guiberti, T.F.; Wang, J. Flame stabilization and emission characteristics of ammonia combustion in lab-scale gas turbine combustors: Recent progress and prospects. *Prog. Energy Combust. Sci.* **2025**, *106*, 101193. [CrossRef]
129. Liu, J.; Wu, Q.; He, K.; Kang, X.; Shi, X.; Zhou, H. Experimental study on pollutant emissions and fly ash characteristics in ammonia-bituminous coal co-firing under different ammonia injection modes in a swirl burner. *J. Energy Inst.* **2025**, *123*, 102265. [CrossRef]
130. Elbaz, A.M.; Wang, S.; Guiberti, T.F.; Roberts, W.L. Review on the recent advances on ammonia combustion from the fundamentals to the applications. *Fuel Commun.* **2022**, *10*, 100053. [CrossRef]
131. Mackrory, A.J.; Tree, D.R. Measurement of nitrogen evolution in a staged oxy-combustion coal flame. *Fuel* **2012**, *93*, 298–304. [CrossRef]
132. Wang, X.; Fan, W.D.; Chen, J.; Zhang, H. Experimental study of effect of a novel ammonia/coal co-firing mode on NO_x emission under high temperature conditions. *Renew. Energy* **2024**, *235*, 121379. [CrossRef]
133. Zhang, W.; Liu, X.; Zhang, C.; Li, M.; Niu, T.; Xie, Y. Industrial scale testing on the combustion and NO_x emission characteristics of ammonia cofiring in a 40 MW_{th} coal-fired boiler. *Fuel* **2024**, *359*, 130471. [CrossRef]
134. Wang, S. The Effect of Co-Firing Ammonia with Coal on The Operation Performance of A 600mw Supercritical Pulverized Coal-Fired Boiler. Master's Thesis, Southeast University, Nanjing, China, May 2023.
135. Tan, J.; He, Y.; Zhu, R.; Zhu, Y.; Wang, Z. Experimental study on co-firing characteristics of ammonia with pulverized coal in a staged combustion drop tube furnace. *Proc. Combust. Inst.* **2023**, *39*, 3217–3225. [CrossRef]
136. Wang, X.; Fan, W.; Chen, J.; Feng, G.; Zhang, X. Experimental study on effects of air-staged strategy and NH3 co-firing ratios on NO formation characteristics in ammonia/coal co-firing process. *Fuel* **2023**, *332*, 126217. [CrossRef]
137. Chen, P.; Fang, Y.; Wang, P.; Gu, M.; Luo, K.; Fan, J. The effect of ammonia co-firing on NO heterogeneous reduction in the high-temperature reduction zone of coal air-staging combustion: Experimental and quantum chemistry study. *Combust. Flame* **2022**, *237*, 111857. [CrossRef]
138. Ammonia Power Breakthrough Achieved: Coal Units to Realize Ammonia Co-Firing Decarbonization. Available online: https://www.news.cn/local/2023-04/08/c_1129505294.htm (accessed on 28 September 2025).
139. Huaneng Xi'an Thermal Power Research Institute Builds New Engine for Green Power. Available online: http://mm.chinapower.com.cn/tanzhonghe/fengcai/2024-12-26/272660.html (accessed on 28 September 2025).
140. JERA Successfully Completes Ammonia Co-Firing Test at Hekinan Power Station. Available online: http://www.china-nengyuan.com/news/212223.html (accessed on 28 September 2025).
141. Liu, X.; Lei, L.; Zhou, Z.; Xu, Y.; Hu, Y.; Xu, M. Research Progress and Prospect of Ammonia-doped Combustion in Coal-fired Power Plants Under the Background of Dual Carbon. *Proc. CSEE* **2024**, *44*, 7221–7235. [CrossRef]
142. Kong, Y.; Hu, R.; Qin, Z.; Lin, W.; Li, L.; Han, H. Research progress on combustion characteristics and technical applications of hydrogen-blended natural gas. *Oil Gas Storage Transp.* **2025**, *44*, 153–167. [CrossRef]
143. Wei, D. Research on Combustion and Nitrogen Oxide Release Characteristics of Coal, Sludge, and Ammonia/Hydrogen Co-Combustion. Ph.D. Thesis, North China Electric Power University, Beijing, China, May 2024.
144. Xv, W. Brief Analysis of Methane Steam Reforming for Hydrogen Production and Its Progress. *China Plant Eng.* **2023**, *7*, 197–198.
145. Shahabuddin, M.; Alam, T. Gasification of Solid Fuels (Coal, Biomass and MSW): Overview, Challenges and Mitigation Strategies. *Energies* **2022**, *15*, 4444. [CrossRef]

146. Zhai, Y.; Miao, C.; Zhuang, X.; Tan, X.; Zhang, Q.; Jin, Z. Research Progress of Hydrogen Production by Dark Fermentation of Biomass. *Biomass Chem. Eng.* **2025**, *59*, 53–62.
147. China's Hydrogen Production and Consumption Scale Ranked First Globally in 2024. Available online: https://www.nea.gov.cn/20250530/a2ec7c8861f14df993ad4b1857bf82b9/c.html (accessed on 28 September 2025).
148. CHD's First 12,000 Nm^3/h Green Hydrogen Demonstration Project Commences Operation. Available online: https://h2.in-en.com/html/h2-2433755.shtml (accessed on 28 September 2025).
149. Sinopec's Xinjiang Kuqa Green Hydrogen Demonstration Project Fully Commissioned, Achieving China's First Large-Scale Industrial Application of Green Hydrogen. Available online: https://solar.in-en.com/html/solar-2427789.shtml (accessed on 28 September 2025).
150. World's Largest Single-Unit Green Ammonia Project Commissions—SPIC Da'an Jidian Green Hydrogen-to-Ammonia Integrated Demonstration. Available online: http://www.daan.gov.cn/daxw/ztbd/202507/t20250728_1018229.html (accessed on 28 September 2025).
151. NASA Ames Research Center in California Installs World's Largest 4MW SOEC Electrolyzer. Available online: https://cn.fuelcellchina.com/Industry_information_details/558.html (accessed on 28 September 2025).
152. Germany Builds the World's Largest PEM Electrolyzer. Available online: https://h2.in-en.com/html/h2-2442204.shtml (accessed on 28 September 2025).
153. Tashkent's Green Hydrogen Project Enters Hydrogen Production Operation Phase. Available online: https://www.powerchina.cn/col/col7449/art/2025/art_719575745.html (accessed on 28 September 2025).
154. Rong, Y.; Chen, S.; Li, C.; Chen, X.; Xie, L.; Chen, J. Techno-economic analysis of hydrogen storage and transportation from hydrogen plant to terminal refueling station. *Int. J. Hydrogen Energy* **2024**, *52*, 547–558. [CrossRef]
155. Cao, Q.; Wang, H.; Qin, Y.; Wang, M. Current Status and Analysis of the Development of Pure Hydrogen Pipeline Hydrogen Transmission Technology. *Mech. Eng.* **2024**, *46*, 18–27.
156. Khan, M.A.; Layzell, D.; Young, C. The Techno-Economics of Hydrogen Pipelines. *Transit. Accel. Tech. Briefs* **2021**, *1*, 1–40.
157. Guo, L. The Development Trend of the Domestic and International Hydrogen Energy Industry and Henan's Path Selection. *China Natl. Cond. Strength* **2022**, *9*, 51–54. [CrossRef]
158. Chen, W.; Shi, Z.; Lin, H.; Zhang, J.; Zhang, S. Analyses and suggestions on current development status of China's green hydrogen industry. *J. Xiamen Univ. (Nat. Sci.)* **2025**, *64*, 193–203+210.
159. Liu, X.; Ren, J.; Li, F.; Li, K. Numerical Simulation of Effect of Primary Air Mixed with Hydrogen and Oxygen on Furnace Temperature of Coal-fired Boiler. *J. Eng. Therm. Energy Power* **2023**, *38*, 156–163. [CrossRef]
160. Colin, S.; de Las Heras, F.J.T.; Normann, F.; Johansson, A.; Fernberg, J.; Sepman, A. Configuring hydrogen lancing to reduce carbon and nitrogen oxides emissions from coal-fired rotary kilns. *Int. J. Hydrogen Energy* **2025**, *120*, 323–332. [CrossRef]
161. Zhao, S.; Wang, Y.; Wang, X.; Wei, G.; Lin, S.; Fan, W. Experimental study on the influence of coal/hydrogen co-firing on combustion characteristics. *Clean Coal Technol.* **2025**, 1–7. Available online: https://link.cnki.net/urlid/11.3676.TD.20240730.0944.002 (accessed on 28 September 2025).
162. Yang, L.; Wang, Y.; Wang, X.; Yang, Z.; Chen, J.; Wei, G. Study on combustion technology of pulverized coal mixed with hydrogen. *Ind. Saf. Environ. Prot.* **2025**, *51*, 104–108.
163. Johansson, A.; Fernberg, J.; Sepman, A.; Colin, S.; Wennebro, J.; Normann, F. Cofiring of hydrogen and pulverized coal in rotary kilns using one integrated burner. *Int. J. Hydrogen Energy* **2024**, *90*, 342–352. [CrossRef]
164. Cen, K.; Yao, Q.; Luo, Z.; Gao, X. *Combustion Theory and Pollution Control*, 2nd ed.; China Machine Press: Beijing, China, 2019; pp. 253–282.
165. Bowman, C.T. Control of combustion-generated nitrogen oxide emissions: Technology driven by regulation. *Symp. Int. Combust.* **1992**, *24*, 859–878. [CrossRef]
166. Yao, Q.; Li, S.; Wang, Y. *An Introduction to Combustion Concepts and Applications*, 3rd ed.; Tsinghua University Press: Beijing, China, 2015; pp. 137–147.
167. Gu, X.; Cheng, M.; Zhang, X.; Zeng, Y. The pollutant discharge improvement by introducing HHO gas into biomass boiler. *Int. J. Hydrogen Energy* **2021**, *46*, 23292–23300. [CrossRef]
168. Zhang, Y.; Wu, Q.; Kang, X.; Hou, B.; Zhu, Y.; Zhou, H. Comparative experimental study on the co-firing characteristics of water electrolysis gas (HHO) and lean coal/lignite with different injection modes in a one-dimensional furnace. *Fuel* **2024**, *378*, 132968. [CrossRef]
169. Zhang, Y.; Wu, Q.; Zhu, Y.; Kang, X.; Hou, B.; Zhou, H. Multiple functionalities of oxyhydrogen gas in bituminous coal co-firing: Experimental validation of emission reduction, enhanced burnout efficiency and particle evolution. *Fuel* **2025**, *401*, 135950. [CrossRef]
170. Hydrogen Co-Firing at Star Brand Energy's Hillabee Power Plant (U.S.): Charting the Future of Clean Energy. Available online: https://www.siemens-energy.com/cn/zh/home/references/constellation-energy-hillabee.html (accessed on 29 September 2025).

171. Sanyou Group Thermal Power Company: How Green Electricity Is Forged. Available online: https://www.tsr.he.cn/xwtj/2024-11/29/cms223808article.shtml (accessed on 29 September 2025).
172. Sánchez-Lozano, D.; Vera, D.; Escámez, A.; Awaafo, A.; Jurado, F.; Vera, D. Techno-economic assessment of a hybrid PV-assisted biomass gasification CCHP plant for electrification of a rural area in the Savannah region of Ghana. *Appl. Energy* **2025**, *377*, 124446. [CrossRef]
173. The Central People's Government of the People's Republic of China. China's Actions on Carbon Peaking and Carbon Neutrality. Available online: https://www.gov.cn/zhengce/202511/content_7047492.htm (accessed on 16 December 2025).
174. U.S. Department of Energy. Energy Department Announces $100 Million to Restore America's Coal Plants. Available online: https://www.energy.gov/articles/energy-department-announces-100-million-restore-americas-coal-plants (accessed on 16 December 2025).

Disclaimer/Publisher's Note: The statements, opinions and data contained in all publications are solely those of the individual author(s) and contributor(s) and not of MDPI and/or the editor(s). MDPI and/or the editor(s) disclaim responsibility for any injury to people or property resulting from any ideas, methods, instructions or products referred to in the content.